# MEASUREMENT OF NONUNIFORM MAGNETIZED ARGON PLASMA DISCHARGE PARAMETERS

A THESIS SUBMITTED TO
THE GRADUATE SCHOOL OF NATURAL AND APPLIED SCIENCES
OF
MIDDLE EAST TECHNICAL UNIVERSITY

BY

EBRU DAĞTEKİN

IN PARTIAL FULFILLMENT OF THE REQUIREMENTS
FOR
THE DEGREE OF
MASTER OF SCIENCE
IN
PHYSICS

DECEMBER 2006

Approval of the Graduate School of Natural and Applied Sciences.

Prof. Dr. Canan Özgen
Director

I certify that this thesis satisfies all the requirements as a thesis for the degree of Master of Science.

Prof. Dr. Sinan Bilikmen
Head of Department

This is to certify that we have read this thesis and that in our opinion it is fully adequate, in scope and quality, as a thesis for the degree of Master of Science.

Prof. Dr. Sinan Bilikmen
Supervisor

**Examining Committee Members**

Prof. Dr. Arif Demir (Kocaeli Univ., PHYS)

Prof. Dr. Sinan Bilikmen (METU, PHYS)

Prof. Dr. Gülay Öke (METU, PHYS)

Assist. Prof. İsmail Rafatov (METU, PHYS)

Dr. Burak Yedierler (METU, PHYS)

**“I hereby declare that all information in this document has been obtained and presented in accordance with academic rules and ethical conduct. I also declare that, as required by these rules and conduct, I have fully cited and referenced all material and results that are not original to this work."**

Name Surname : EBRU DAĞTEKİN

Signature :

## ABSTRACT

MEASUREMENT OF NONUNIFORM MAGNETIZED ARGON PLASMA DISCHARGE PARAMETERS

Dağtekin, Ebru

M.Sc., Department of Physics

Supervisor: Prof. Dr. Sinan Bilikmen

December 2006, 63 pages.

Effects of a magnetic field on the double-probe technique are studied experimentally by means of symmetric floating computer controlled fast double probes in low and intermediate pressure plasmas. In addition, the effects of the magnetic field on the electron temperature, electron density, and electric field have been investigated. As it is expected, when there is no magnetic field, properties of the discharge plasma are best described by Langmuir theory. Whereas, when there's a magnetic field of sufficient strength Schottky's theory of ambipolar diffusion applies.



Keywords: Fast Langmuir probe, electron temperature, electron density, positive column, magnetic field.

# ÖZ

DÜZGÜN OLMAYAN ARGON PLAZMA BOŞALMASINDA PARAMETRELERİN MANYETİK ALAN İÇİNDE ÖLÇÜLMESİ

Dağtekin, Ebru

M.Sc., Department of Physics

Supervisor: Prof. Dr. Sinan Bilikmen

Aralık 2006, 63 sayfa.

Düşük ve orta basınçlı plazmalarda deneysel olarak, manyetik Alanın İkili prob tekniği üzerine etkileri simetrik yalıtılmış bilgisayar kontrollü hızlı çift prob yoluyla çalışılmıştır. Bununla birlikte manyetik alanın elektron sıcaklığına, elektron yoğunluğuna ve elektrik alanına etkileri araştırılmıştır. Manyetik alan mevcut değilken Langmuir' in serbest iyon düşme teorisi boşalmalı plazma sisteminin özelliklerini en iyi biçimde tanımlarken, yeterli güçte manyetik alanın varlığında, Schottky'nin ambipolar difüzyon teorisi geçerlidir.

Anahtar Kelimeler: Hızlı Langmuir prob, elektron sıcaklığı, elektron yoğunluğu, pozitif kolon, manyetik alan.

...TO MY FAMILY

## ACKNOWLEDGEMENTS

I am grateful to all who have helped me to have the opportunity and possibility to continue the graduate study and to prepare this thesis. My sincere gratitude and deep appreciation to Prof. Dr. Sinan Bilikmen for his kind assistance and supervision. I wish to thank Dr. Demiral Akbar for his guidance in the plasma lab and all staff of electronic laboratory, to my graduate friends and my mother for her eternal patience and support.

## TABLE OF CONTENTS

## LIST OF FIGURES

FIGURES

# CHAPTER 1

# INTRODUCTION

DC glow discharges have been used for plasma processing applications in the low and intermediate pressure regimes in modern technology.

Because plasmas are conductive and respond to electric and magnetic fields and can be efficient sources of radiation, they are usable in numerous applications where such control is needed or when special sources of energy and radiation are required [1].

The development of plasma science in the past three decades has been propelled by applications such as fusion energy, space science and the need for defense, and this support has resulted in significant progress [2].

The electric fields in the low temperature plasmas can reveal significant energy to the electrons and ions but the plasmas are still cool enough to support a multitude of chemical reactions, and they are critical to the processing of many modern materials such as the fabrication of semiconductors. The plasma etching for semiconductors and the surface modification and growth of new materials are some of the important examples.

Other important uses of low temperature plasmas include the “cold” pasteurization of foods, the sterilization of medical products, environmental cleanup, gas discharge for lightning such as fluorescent lights and lasers, isotope separation, switching and welding technology, and plasma-based space propulsion systems.

The main working parameters-temperature and pressure of the vast majority of technological processes are unavoidably increasing and therefore nowadays we can mention from a Renaissance. It follows that more and more considerable part of a processed material converts into the plasma state and an opinion arises that in the coming century the considerable, if not the main, part of the materials and surface processing will inevitably use the plasma technology.

The second reason of extreme rise of interest in this field follows from the fact that, among the more or less easily obtainable objects, the low temperature gas discharge plasmas are the most remote ones from the thermodynamic equilibrium. As a result, a great variety of the plasmas are widely used as active media of optical quantum generators and amplifiers. This extremely non-equilibrium property of the plasmas are widely used as active media of optical quantum generators and amplifiers. This also is the reason why the most exotic chemical synthesis, which cannot be performed otherwise, is possible in the plasma state [3].

The main part of plasma science presently practiced in this domain is gaseous electronics-based. In its original configuration, the gas discharge branch of Langmuir's plasma physics, founded in the early part of this century, focused on electron conduction and breakdown in gases, electron emission and other cathode phenomena, and excitation of atomic and molecular species by electron collisions.

Applications of the physical principles derived in this new field of science developed rapidly, beginning with the carbon used as light source and followed by gas-discharge rectification, high-power switch gear and welding arcs. The pervasive use of plasmas in modern technology is a result of the range of parameters that can be accessed and that is inaccessible by any other means. No other medium can provide gas temperatures or energy densities as high as those of plasmas: no other medium can excite atomic or molecular species to radiate as efficiently; no other medium can be arranged to provide comparable transient and nonequilibrium conditions [4].

Time is an important boundary limited agent in quantifying plasma parameters especially ion currents and assembling data in a few seconds effects the results. With the help of three couples of double probe system measurements has been taken. The experiment is realized with using input/output data acquisition/control board (NI 6014) from National Instruments connected to a personal computer (PC). The time resolution of the system has a maximum value of 5 μs.

In this study taking into consideration of double Langmuir probes system advantages, such as double probe system does not require the presence of a grounded reference in contact with the plasma, it is used instead of single probe system. Another advantage is that the total collected current is limited with the ion

saturation current. The behavior of the magnetized plasma is determined largely by the configuration of the magnetic field in the plasma. Currents and plasma flows can induce changes in the topology of the field by breaking and reconnecting the magnetic field lines. Our aim is to illustrate the way that magnetic field affect the plasma, how organizes it again and converts nonmagnetized plasma parameters into magnetized ones.

# CHAPTER 2

# DC GLOW DISCHARGE

## 2.1 Basics

The regions of an active discharge in gases at low pressure were extensively studied and characterized at an early stage in the development of physics. A simple experiment can demonstrate several essential types of discharge. The tube can be evacuated and filled with several gases at different pressures. The voltage between the electrodes and the current in the circuit will be measured. If a voltage of a few tens of volts is applied to the electrodes, no visible effects are produced. However, an extremely sensitive device would record a very low current on the order of $10^{-15}$ A due to charges generated in the gas by cosmic rays and natural radioactivity. The field pulls them to the opposite-sign electrodes, producing a current. If the gas is deliberately irradiated by a radioactive or an X-ray source, a current on the order of $10^{-6}$ A can be produced. The resultant ionization of the gas is still too small for emitting light.

We can describe a discharge as non-self-sustaining when an electric current survive under the conditions of an external ionizing agent or the emission of electrons or ions from electrons is maintained (e.g. by heating the cathode). An additional increase of voltage increases the current sharply until a certain value of V and light emission is remarked. These are indications of breakdown, one of the important discharge processes. At a pressure $p \approx 1$ Torr and inter-electrode separation $L \approx 1$ cm, the breakdown voltage is several hundred volts. A small number of artificial electrons or electrons injected intentionally to stimulate the process starts breakdown: The discharge immediately becomes self-sustaining. During their motion the energy of the electron increases and after reaching the atomic ionization potential, the electron spends this energy by colliding with another electron. Two slow electrons are thus produced, which go on to repeat the

cycle described above. The result is an electron avalanche. The gas is appreciably ionized in $10^{-7}$ to $10^{-3}$ s, which is sufficient for the current to grow by several orders of magnitude. At low pressure and high resistance of the external circuit (it prevents the current to reach a large value), a glow discharge develops.

We can classify the discharges regarding the uniformity of electric field in two classes:

1- At low current densities (i.e. charge carrier densities) the electric field due to the space charge can be neglected and it is uniform. The electric field can be found by V/d, where d is the distance between the electrodes.

2- At high current densities the electric field due to space charges will become important and as a result the total electric field will be non-uniform. The electric field distribution has to be calculated by means of Poisson's equation:

$$\vec{\nabla} . \vec{E} = \left( \frac{e}{\varepsilon_0} \right) (n_i - n_e) = \left( \frac{\rho}{\varepsilon_0} \right) \qquad (2.1)$$

where

e = charge of the electron

$\varepsilon_0$ = permittivity of the free space

$n_{e,i}$= number density, for electron and ions

$\rho$ = space charge density = e ($n_i$ - $n_e$)

The so – called electrical characteristic of the discharge is described by the I-V curve as shown in Figure (2.1). It is determined by the external parameters p, d, the electrode material, the gas type and the external current density. The desired operating point is fixed by the choice of the external resistance R.

The electrical characteristic can be subdivided into three regions:

1-The low current region, I < $10^{-6}$ A; the range of the Townsend discharge; because little or no light is emitted it is also called "dark discharge". The electric field is uniform.

2-With $I \geq 10^{-6}$ A; the electric field configuration changes due to the onset of space charge distortion. The potential drop $V_C$ is confined to a short region in front of the cathode (cathode fall). For a certain range of the current the voltage drop $V_C$ is independent of the current, this is the so called normal glow discharge region. With increasing current $V_C$ rises; we enter the region of abnormal glow.

3-Further increase of the current leads to the so-called glow-to-arc transition. The cathode fall undergoes a transformation from cold cathode discharge to a hot cathode discharge with thermionic emission.

In this work, we are interested in region 2 of the plasma characteristic. The plasma parameter ranges are:

$10^8$ cm$^{-3} \leq n_e \leq 10^{12}$ cm$^{-3}$ , $10^{-4}$ torr $\leq p \leq 10$ torr, 0.1 eV$\leq T_e \leq 10$ eV, and

5 x $10^{12}$ cm$^{-3} \leq n_g \leq 3$ x $10^{17}$ cm$^{-3}$; i.e. $n_e/n_0 \approx 10^{-6} - 10^{-3}$ and $\lambda_D \approx 10^{-2} - 10^{-1}$ cm. Where $n_g$ denotes the density of the neutral atoms, $T_e$ the electron temperature, and $\lambda_D$ is the Debye length ($\lambda_D$(cm)=743 $(T_e/n_e)^{1/2}$) with $T_e$ in electron-volts and $n_e$ in cm$^{-3}$[12,10].

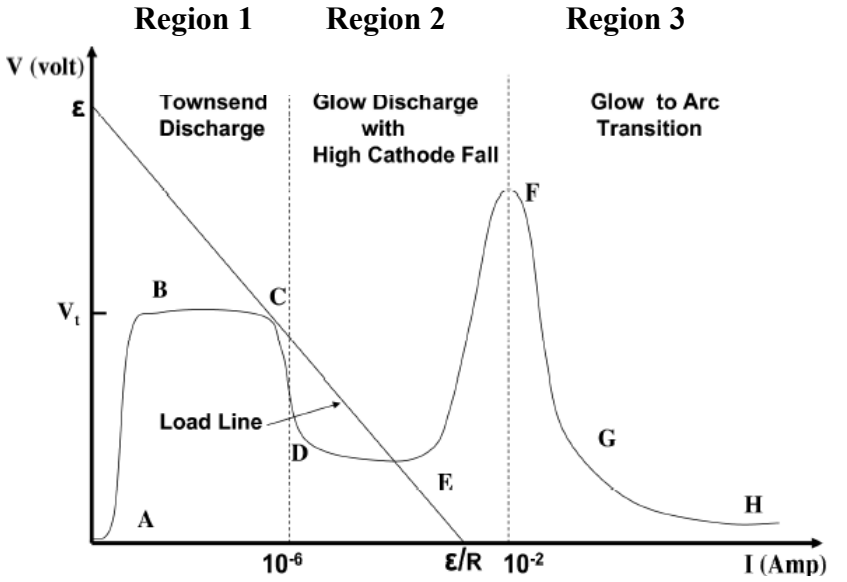

Figure 2.1: Schematic I-V curve of a glow discharge [16].

The glow discharge gets its name from a luminous zone which develops near the cathode and is separated from it by a dark space. The ionized gas in the column is electrically neutral practically everywhere except for the regions close to electrodes. Therefore, it is called as plasma. From the aspects of two main criterions, which are first the state of the ionized gas and second the frequency

range of the field, glow discharge can be classified as non-equilibrium plasma with constant electric field.

The essential supply of electrons is obtained mainly from secondary emission caused by the bombardment of the cathode by positive ions, that is, by action of the current itself. It is conveniently described as a discharge in which the cathode emits electrons under the bombardment of particles and light quanta from the gas.

A characteristic property of glow discharge is a layer of large positive space charge at the cathode, with a strong field at the surface and considerable potential drop of 100-400 V (or more). This drop is called as cathode fall and the thickness of the cathode fall layer is inversely proportional to the density of the gas. In this case the inter-electrode separation is sufficiently large; an electrically neutral plasma region with weak field is established between the cathode and anode layers. This relatively homogeneous part is called positive column. The anode layer exists between positive column and the anode.

The positive column constitutes weakly ionized non-equilibrium plasma-that is, an ionized gas having no net space charge. It serves only to maintain the conduction of current by electrons which are established in the cathode region.

It is known that there are a variety of glow discharges and their appearance varies with the nature of the gas, pressure, type and size, separation, material of the electrodes and the radius of discharge tubes (e.g. narrow, capillary, rectangular and cylindrical). The comparisons between these kinds of vessels have been investigated separately by numerous authors [5, 6, 7, 8].

In many uniform dc glow discharge systems [9, 10, 11, 12], the electron density is small near the cathode and increases towards the anode because of ionization of electrons. In other words, the electron temperature increases sharply near the cathode and remains constant near the anode. Also, the axial component of the electric field is constant in the uniform positive column.

## 2.2 General Characterization of DC Glow Discharges

The appearance of a gas changes when the electric discharge passes through it at a low pressure differences and various points in its path become very clearly marked.

Basically, a source of electrons or cathode, let it be a cold metal plate, must exists and it should emit secondary electrons because of ion bombardment, impart of meta-stable gas atoms, or sufficiently energetic ultraviolet radiation, or a hot thermionicaly emitting surface can serve for this. The conditions near the cathode are determined by the immediate electrical potential drop in front of the cathode and also by the ion bombardment which ion bombardment a sufficient yield of electrons appears.

At the cathode strong fields excite the electrons and they are accelerated until they reach to energies greater than the optimum value for ionization. Therefore, regions in which the initial electrons are scattered and lose energy until the motion is randomized and an optimum situation is achieved.

Under these conditions, it is possible to build a balance between the gain of the energy input from the longitudinal field and the loss of energy due to inelastic collisions with the gas atoms, between the particle-generation process of ionization of the gas atoms by electron impact and the loss process due to particle interaction with the walls. The loss process arises because there are radial electric fields caused by the charged particles which lead to their motion in a radial direction and may be treated as free flight at very low pressures or diffusive at moderate pressures, particles of opposite sign then recombining on the wall. At high pressures when the reduced fields are low, recombination in the volume is an important process [13].

In a long cylindrical tube which includes a rare gas at a pressure between 0.1 and 1 mm Hg, a discharge occurs and visible light is emitted from the tube. At the very beginning of the tube close to the cathode there exists sometimes a very narrow dark space (Aston`s ) and it is followed by a thin relatively feeble sheath luminous layer-the cathode glow- which in turn is followed by the cathode dark space. Aston`s dark space and the cathode glow can not always observed clearly.

The negative glow is separated with a sharp boundary from the cathode dark space and the negative glow becomes progressively dimmer towards the `Faraday

dark space`. The positive column is at the positive end of it and is either a region of uniform luminosity or regularly striated. Increasing pressure leads the positive column contracting radially.

Sometimes a visible anode dark space exists at the positive end of the positive column and it depends on the gas and the value of the discharge current. The relative light intensities are shown in Figure (2.2a). The distribution of the applied voltage along the discharge is shown in Figure (2.2b). Three parts in the discharge may be distinguished, a cathode fall, an anode fall and a part where the electric field (E) is constant "positive column". Most of the applied potential is required for the cathode dark space when the field is high as indicated in Figure (2.2c). The discharge current is mainly electronic rather than ionic because of the greater mobility of the electrons. The current density and net space charge density distribution along the discharge are shown in Fig. (2.2 d and f) respectively [14].

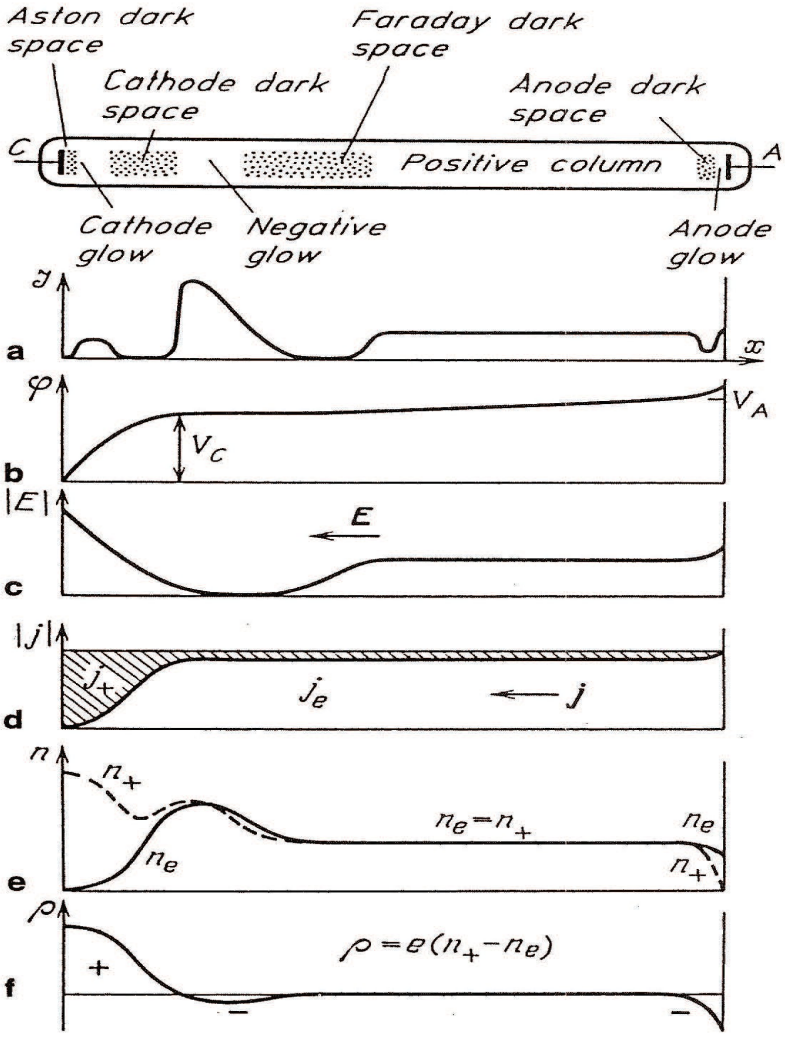


Figure 2.2: Classification of the glow discharge [16]

## 2.3 The Cathode Region

Positive-ion bombardment is the main factor for maintenance of the discharge at the cathode. A positive ion with a greater total energy than twice of work function required for removing of an electron, then one electron may be ejected while a second neutralizes the ion.

An ion or atom with energy equal to twice the ionization energy has the ability of ionizing an atom it strikes. Ion velocity and the kind of gas, electrode material can increase the probability of this event, measured as $\gamma_i$, the yield of electrons per incident ion. The escape of electrons can be prevented by maximum depth of penetration when ion reaches high energies like $10^5$ eV.

The electrons near the cathode surface form a negative space charge, before they gain appreciable velocity, but since they are then accelerated by the electric field and since in any case the current is mostly due to positive ions in this region, the space charge becomes positive a short distance from the cathode and remains positive ions in this region and remains positive through the cathode dark space.

Between the cathode and Aston dark spaces the cathode glow exists and has a reddish color and is due to the recombination of incoming positive ions with slow electrons, for which the recombination coefficient is high. A larger voltage gradient can occur because of the large net positive space charge formed in the cathode dark space, so most of the tube voltage is taken up here and the electrons are accelerated sufficiently to produce intense ionization and therefore multiplication. By the end of the cathode dark space, the current is nearly all carried by the electrons, whose numbers are then so great, despite their high average velocity, they considerably reduce the net positive space charge [15].

The axial length of the negative zones i.e. those near the cathode, are independent of the distance between anode and cathode of a glow discharge but the length of the positive column changes.

## 2.4 The Negative Glow and Faraday Dark Space

The density of electrons at the anode side of the cathode dark space is increased at the points at which there are sufficient electrons to carry the entire

current and to make the net space charge negative. When the sign of the space charge reverses just before the voltage gradient becomes slightly negative, reaching a negative maximum, the acceleration of fast electrons emerging from the cathode dark space ends and their energy is absorbed mainly by intense excitation and ionization – the reason of the brightness of the negative glow. As the electrons are slowed down the negative space charge reaches a maximum, the energy available for excitation and ionization is exhausted and the Faraday dark space begins, there is no sharp boundary. The electron density decreases by recombination and diffusion in the dark space until the net space charge becomes zero again and E attains a constant small value, at which point the positive column begins. [15]

## 2.5 The Positive Column

Bounded at one end by the Faraday dark space and at the other by the anode glow is the positive column. It is so called because it connects the negative zones to the anode; usually it is produced in cylindrical tubes, though a "positive column" can no doubt be obtained between two parallel walls.

The positive column is not really necessary for maintaining a glow discharge, although it can be the largest part of the discharge. In long tubes, as for example neon signs, the positive column may be straight or bent and have any length provided the applied voltage is sufficiently high. The column is usually uniform, as can be seen from the constancy of the axial potential gradient or the constant average energy of electrons at any point (unless the geometry varies). Also the radiation emitted per unit axial length is everywhere the same and any chemical changes occur along its length.

The axial gradient dV/dx can be found by observing the potential difference between two probes placed at a known distance apart or by reading the voltage across the discharge for constant current and varying electrode distance. Because dV/dx = constant, thus from Poisson's equation the number of positive and negative charges per unit volume or per unit length of column is equal. The main principle is that the positive column serves to maintain the conduction of current by electrons which are established in the cathode region.

Basically, it closes the electric circuit in the space between the cathode layer and the anode. The regions adjacent to the electrodes do not affect the state of the plasma in a sufficiently long column. It is determined by local processes and by the electric current the inevitable loss of charge carriers (electrons) in the column must be compensated by ionization. Since the ionization rate depends on the field strength E through the dependence of electron energy distribution, the field necessary for sustaining stationary plasma is fixed. This determines the longitudinal potential gradient and the voltage difference across a column of a given length. If the electron energy density spectrum is a Maxwellian, the relationship can explained into two causally linked parts:

1- The requirement of the loss compensation by ionization shows what the electron temperature $T_e$ should be.
2- The field must supply the necessary energy to the electrons.

The creation and removal of electrons in the column proceed against a steady background of unceasing electron replacement due to the drift motion from the cathode to anode.

It can not be said that a considerable fraction of charge carriers are generated in the glow discharge column. Rather, the majority of electrons reaching the anode enter the column from the outside (from the cathode region). The probability for them to be lost on the way is not so high, except for cases of exponentially long inter-electrode separations. The gas temperature $T_{gas}$ is determined by the balance of the gas energy as a whole. In the positive column of glow discharge, we have $T_e >> T_{gas}$ [16].

### 2.5.1 Theory of Positive Column in the absence of Magnetic Field

The positive column, which is namely a typical plasma, contains equal concentration of positive ions $n_+$ and negative ions $n_-$ and / or electrons $n_e$ , each with its velocity distribution and characteristic temperature. Following Schottky's theory [20] we assume that there are many electron collisions along the tube radius R, that is the electron mean free path is greater than the tube radius $\lambda_e \gg R$.

Ionization in the gas occurs only by single collision between fast electrons and gas molecules. The number loss is due to ambipolar diffusion. A single

collision between the fast electrons and gas molecules is resulted with ionization of the gas. The number of loss is due to ambipolar diffusion, thus both electrons and ions move with the same speed radially outwards. The electrons and positive ions neutralize their charge on the wall because they do not recombine in the gas. Therefore, their concentration is large at the axis and is practically zero on the insulated wall. We have therefore in any volume element of the column the same number of positive and negative charges, but this number is different in volume elements which are not at the same distance from the axis.

Schottky diffusion theory can explain the radial distribution of the electron and ion densities. It is well known that the positive column spreads laterally to the wall at pressures less than a few Torr for the large discharge currents.

The Schottky theory well describes the spread positive column where the direct ionization balances with the diffusion in the whole plasma. He developed an ambipolar diffusion theory in which he assumed quasi-neutrality of the plasma and neglected the effect of charged particle inertia on the radial structure of the positive column.

Many researches show that the radial electron distribution is usually close to the $J_0$-Bessel function. In this theory, electrons are in equilibrium with the axial electric field, implying that the energy imported to the electrons by a steady uniform electric field is exactly balanced by energy lost in elastic and inelastic collisions with heavy particles in each volume element of the discharge [21, 42].

The special features of the electron motion in the potential field of the positive column are related to their acceleration in the longitudinal field, and their deceleration in the radial field. The axial electric field drives the discharge current $I_d$ and yields the power input to the plasma, which is mainly absorbed by the electron components.

However, the radial electric field is caused by the establishment of space-charges and can reach more than 100 V/cm near the dielectric walls. It accelerates the ions and retards electron movement toward the wall, in such a way that ambipolar radial flux of electrons and ions is established [22, 43]. At low pressure, when the total energy is conserved electron motion in the radial direction occurs. In case the radial electric field is larger than the axial field as in electrons with large

radii, they are accelerated by the axial electric field to kinetic energy below the ionization potential.

The electrons move radially inward at nearly constant energy, and by ambipolar electrical field they are accelerated above the ionization threshold. The lower-energy electrons move radially outward after undergoing the elastic ionization collision.

Since electrons have smaller mobility and drift velocity compared to the ions, the current in the positive column is mainly carried by electrons. An accumulation of positive charge will increase with time, because an equal number of charges of both signs are produced in the column, but there is a constant influx of electrons from the Faraday dark space which constitutes the current. The anode removes the electrons to the positive end of the column. Ionization in the anode region by the field of the anode also creates a constant flow of positive ions down the column. As a result of ionization in the anode region, electrons are driven into the positive column by the field of the anode. A well defined quantitative description of the relations between the axial and radial electric field, the pressure, the tube radius, and the nature of the gas can be given with the elementary theory of the positive column. The following assumptions were used when the particle density equations have been derived:

(i) The Debye length and the electron mean free path are sufficiently smaller than the discharge tube radius.

(ii) The radial density distributions of the particles are homogeneous.

This means that the plasma density at the tube wall can be regarded as zero and the ion sheath thickness at the wall can be neglected. Assumption (ii) is valid to the first approximation for both electrons and ions and was often used in the theoretical studies of positive column, when the process of ambipolar diffusion is dominant [23, 24, and 25]. Experimental results show that assumption (ii) is also almost valid for the metastable atoms except for the case of (Ne) gas at high pressures [26,42].

Using the assumption that ionization rate and diffusion loss are equal:

( $\lambda_e \ll R$ , $n_+ = n_e = n$, and $(\frac{dn_+}{dr}) = (\frac{dn_e}{dr}) = (\frac{dn}{dr})$ ), where R is the radius of the discharge tube , and r is any radial position from the axis of the tube, in a along

cylindrical positive column a differential equation for number density can be found directly from Laplace's equation by using cylindrical coordinate with symmetric condition around θ, in the form of:

$$\frac{d^2n}{dr^2} + \frac{1}{r}\frac{dn}{dr} + \frac{z}{D_a}n = 0 \qquad (2.2)$$

where z is the number of ionizing collisions per second, and $D_a$ is the ambipolar diffusion coefficient. Without the term zn and with boundary condition n=0 at r =R, the solution of Equation (2.2) is a Bessel function of zero order:

$$\frac{n_r}{n_0} = J_0\left(2.405\ \frac{r}{R}\right) \qquad (2.3)$$

where $n_0$ and $n_r$ are concentration of the charge at the axis and at a radial distance r from the axis ( the concentration of charges in a column varies with r in a nearly parabolic manner), respectively. In addition, in the condition of equality of ionization frequency and the effective frequency of diffusion loss [20, 42]:

$$\nu_i(E) = \frac{D_a}{\Lambda^2} \equiv \nu_{da},\ \Lambda = R / 2.4 \qquad (2.4)$$

where $\nu_i n = -D_a\left(\frac{1}{r}\frac{dn}{dr}\right)$

The case $zn \ll \nu_{da}$ is realized at low pressure and small transverse dimension ($\nu_{da} \propto 1/p\Lambda^2$), at not too high currents, so that n is moderate; it is facilitated in monatomic gases where the bulk recombination proceeds slower than in molecular gases.

If $zn \gg \nu_{da,}$ the recombination of charges in the bulk dominates over their diffusion to the walls. If the diffusion term in Eq. (2.2) is dropped, we find $\nu_i (E) = zn$ , that is , the density is constant over the cross section. In fact a large gradient of n appears at the absorbing walls, and the diffusion there cannot be neglected. Electron or ion density changes only slightly near the center of the discharge tube but drops sharply near the walls [16].

The voltage gradient E in the positive column is given by balancing the energy that the electrons gain energy from the electric field per second and the energy they lose by collisions per second, when collision is elastic it is represented by $l_{elastic}$ and inelastic it is represented by $l_{inelastic}$. Therefore:

$$eEv_d = l_{elastic} + l_{inelastic} \tag{2.5}$$

where

$$l_{elastic} = P\int_0^{\infty} G_{elastic} \frac{m\nu_e^2}{2} \frac{\nu_e}{e} f(\nu_e) d\nu_e \tag{2.6}$$

and

$$\eta = \frac{q_{inelastic}}{(q_{elastic} + q_{inelastic})} \tag{2.7}$$

$$L_i = P\int_0^{\infty} eV_c \eta \frac{\nu_e}{e} f(\nu_e) dv_e \tag{2.8}$$

where $f(\nu_e)$ is the velocity distribution function, $\lambda_e$ mean free path of the electron, $\eta$ ionization and excitation function, $V_c$ critical potential, $\nu_e$ drift velocity, $G_{elastic}$ the energy lost in elastic collision, e and m are electron charge and mass, respectively; P is the pressure, and $T_e$ the electron temperature. Assuming the electron mean free path to be independent of energy, we have ($T_e$ α E / P), if collision frequency is assumed to be constant, we have ($T_e$ α $(E / P)^2$ ).It was shown that except at very low pressures, the electron drift velocity is much lower than the random one, under the conditions exactly corresponding to the glow discharge positive column. Roughly speaking, the electron spectrum is said to be Maxwellian if the frequency of the electron -electron collisions are appreciably higher than the energy loss frequency [12,16,42]. From the equation of ambipolar flow,

$$\nu_a = -\frac{D_+}{n}\frac{dn}{dr} + \mu_+ E = -\frac{D_e}{n}\frac{dn}{dr} - \mu_e E \tag{2.9}$$

the radial field:

$$E_r = \frac{1}{n}\frac{dn}{dr}\frac{D_+ - D_e}{\mu_+ + \mu_e} \approx \frac{1}{n}\frac{dn}{dr}\frac{kT_e}{e} \tag{2.10}$$

and then the potential can be found as:

$$-V_r = \frac{kT_e}{e} \ln \frac{n_0}{n_r} \tag{2.11}$$

or

$$\frac{n_r}{n_0} = \exp\left\{ -\left( \frac{eV_r}{kT_e} \right) \right\} \tag{2.12}$$

Showing that the concentrations of charges follow Boltzmann distribution [12,42].

### 2.5.2 Theory of Positive Column in Magnetic Field

The theory of probes in zero magnetic field rest on two assumptions,

(i) The dimensions of the probe are small compared with the mean free path of ions and electrons. This means that the probe can be assumed to collect only a relatively small number of charged particles in the plasma around the sheath, so outside this sheath the plasma is, to a close approximation, undisturbed by the presence of the probe.

(ii) The thickness of the space charge sheath surrounding the probe is small compared with the mean free path of ions and electrons. Thus the sheath can be treated as a region in which ions and electrons move as in vacuum, undisturbed by collisions.

With a probe collecting across the magnetic field the validity of assumption (ii) depends on the sheath thickness *d* and thus on the plasma density *n,* the type of gas and on B. If (ii) holds, the motion of the charged particles is complicated by the presence of the magnetic field. When (ii) is not valid, electrons make collisions in the sheath. The net flow across the sheath can be neglected and the spatial distribution of the electrons follows Boltzmann's law for particles diffusing in a potential field, assuming that the velocity distribution of the electrons is Maxwellian. The presence of the magnetic field does not invalidate this law. Thus Equation 2.12 is valid.

The effect of an axial magnetic field is typically markedly different for electrons and ions, and depends on the ratio of the appropriate cyclotron frequency to collision frequency [17].

The electron momentum equation is

$$(Z + f_e)\,\vec{v}_e = -e\frac{\vec{v}_e \times \vec{B}}{m} - \frac{e}{m}\vec{E} - \frac{k_B T_e}{m}\frac{\vec{\nabla} n_e}{n_e} \qquad (2.13)$$

where $f_e$ corresponds to electron frequency, Z to atomic number, and $n_e$ to electron density.

If we assume $\vec{B}$ in z- direction and $\vec{E}$ in x-direction and also the variation of $n_e$ and E only in the x – direction then the equation becomes

$$\frac{k_B T_e}{m n_e}\frac{dn_e}{dx} = -\frac{eE}{m} - v_{ey}\frac{eB}{m} - (Z + f_e)v_{ex} \qquad (2.14)$$

and

$$0 = v_{ex}\frac{eB}{m} - (Z + f_e)v_{ey} \qquad (2.15)$$

and the x motion can be found by substituting (2.14) in (2.13) to be given by

$$(Z + f_e)\,v_{ex}\left\{1 + \frac{\omega_{ce}^2}{(f_e + Z)^2}\right\} = -\frac{eE}{m} - \frac{k_B T_e}{m n_e}\frac{dn_e}{dx} \qquad (2.16)$$

The effective electron diffusion coefficient in isothermal plasma is thus

$$D_{em} = k_B T_e \Big/ \left[ m(Z + f_e)\left\{1 + \frac{\omega_{ce}^2}{(f_e + Z)^2}\right\}\right] \qquad (2.17)$$

and is thus reduced by a factor

$$\left\{1 + \frac{\omega_{ce}^2}{(f_e + Z)^2}\right\}\left(1 + \frac{Z}{f_e}\right) \qquad (2.18)$$

in comparison with the magnetic field and ionization – free case, Customarily this is written in the form where the ionization is ignored for weakly ionized plasma Z→ 0 [17, 44], i.e.

$$D_{em} = \frac{D_{e0}}{\left(1 + \left(\omega^2_{ce} / f^2_e\right)\right)} \tag{2.19}$$

when ω=0 magnetic field is zero, $D_{em}= D_{e0}$.

# CHAPTER 3

# ELECTRICAL LANGMUIR PROBE

## 3.1 Overview of Langmuir Probes

Irving Langmuir invented electrostatic plasma probes in the year 1924. The devices which he were developed relatively simple and the first plasma diagnostic instruments also still bear his name, as electrostatic probes are most commonly referred to as "Langmuir probes". Electron density, ion density, electron temperature, plasma potential and floating potential can be measured by probes. The exactness in measuring these plasma properties rely on the particular condition in which they are utilized. Their function is limited to cool plasmas which will not melt or rapidly erode their surfaces because they are material probes that must be inserted into the plasma. From the aspect of construction and operation they presents simple methods, but the interpretation of their data can be quite complex [27].

The Langmuir probe can be interpreted from an experimental point of view as a simple current collector surface immersed into the plasma environment. Many different types of probes were developed and used with success in the case of practical applications. Emissive probes, double probes, capacitive probes, oscillation probes, probes in flowing or high pressure plasmas, and probes in a magnetic field are some examples. Our measurements were carried out using cylindrically shape double probes with 0.175 mm base diameter and 0.5 mm height, made of tungsten wire. The wire must be well insulated for preventing take-current collection. Since the Langmuir probe gives local plasma information it must be mobile and could be locate to any desired point of plasma (radially) chamber's volume.

The probe technique has a main privilege from almost all other techniques such as spectroscopy or microwave propagation, which gives information averaged

over a large volume of plasma. Probe technique gives possibility to acquire local information through measurements [28].

### 3.2 Probe Theory

Usually Langmuir probes consist of one or more metallic, conducting electrodes immersed into plasma. Simply "The Langmuir probe" is a single electrode where one conductor is inserted into the plasma. A characteristic property of the probe is that it is a conducting wire made out of a high temperature metal such as tungsten or nickel, and is enclosed by an insulating sleeve, usually made out of a ceramic such as alumina. The conductor expands out of the insulator some distance to form the probe area. The flow of charge carriers to an electrical probe can be an extremely complicated one. The requirements to apply the electrical probe method to such a wide scope of plasma introduce much analysis. This type of gas discharge is applied by a simplified introduction to the electrical probe method, as given here. The following assumptions are made:

1- The number densities of electrons and ions are equal.
2- Electron and ion mean free paths are much larger than the probe radius.
3- Probe radius is much larger than the Debye length.
4- There is a Maxwellian distribution of electron and positive ion velocities.
5- Electron temperature ($T_e$) is much larger than the positive ion temperature ($T_i$) or ($T_{gas}$).

We can define low pressure plasma as one in which a probe of sufficiently small diameter produces a negligible disturbance to the carrier concentration and in which the great majority of the applied probe to plasma potential is developed across a region that is much thinner than the carrier mean free path [29].

In the low density region, it is an ordinary practice in the industry to use the Orbital Motion Limited (OML) theory of ion collection. Although this theory can be applied successfully well outside its intended range, its error will be greatly increased at higher density. In case probe radii (r) is much smaller than the Debye length $\lambda_D$ (thick sheath), and if the potential around the probe decreases more slowly than $r^{-2}$, we are in the Orbital Motion Limit (OML) region [30].

In this region, ion energy distinguishes itself with an ion impact parameter that makes the ion hit the probe with a grazing, or tangential incidence. A simple function depending on the ion initial energy and the probe potential with respect the plasma defines the maximum impact parameter for hitting the probe. When ($r_p$=D) increases the OML may break down, where $r_p$ is the probe radius and $\lambda_D$ is Debye length ($\lambda_D$ (cm) = $743(T_e/n_e)^{1/2}$) $T_e$ in volts and $n_e$ in $cm^{-3}$. Since the diameter of our probes is (0.175 mm) less than 0.2 mm the OML can be used [31, 32].

### 3.3 Electrical Probe at Low Pressure Discharge

#### 3.3.1 Single Probe

Different shapes of probes exist such as planar, spherical, and cylindrical. Since a definitive theory describing the attitude of the sheath around the probe and the ion current expansion exists, in practice often cylindrical probes are used.

Therefore the measurement of positive ions at highly negative voltages and the calculation of the fast electron current to the probe are allowable. Secondly, in this way it is possible to use small area probes and thus reduce the effects due to depletion of low-energy electrons.

Single Langmuir probe measurement of electron temperature is generally straightforward; on the contrary the measurement of plasma density is more difficult and contains larger experimental errors. A small error in the estimation of the plasma potential can result in a large error in the density measurement since the current below the plasma potential has an exponential dependence on voltage. Since the low energy electrons are reflected the current collected at the plasma potential is also strongly influenced by probe cleanliness. There exists limitations for analytical solutions of the functional dependence on the voltage and therefore using the electron saturation current of the relation probe radius is difficult. The conditions are $r_p/\lambda << 1$ [33, 34].

Therefore the fast computerized three couples of double probe system (TCDP) has been developed and used in our system.

### 3.3.2 Double Probe

In a system composing of two electrodes, referred to as a "double" Langmuir probe, they are immersed into the plasma near each other so that they sample the same plasma properties. Initially both electrodes are floating at potentials below the plasma potential. For applying a potential difference between the two electrodes, a power supply is connected between them. While the current between the probes is recorded, the potential difference is varied using the power supply.

Since a double Langmuir probe instead of a simple Langmuir probe generates the possibility keeping the plasma disturbances to a minimum via only a very small net current drawn from the surrounding plasma, double probe system has advantages. The current collected in one electrode must be taken from the other electrode and this fact constrains the current to the double Langmuir probe. Thus one end of the system is always limited in drawing the ion saturation current at maximum, which tends to be a very small current.

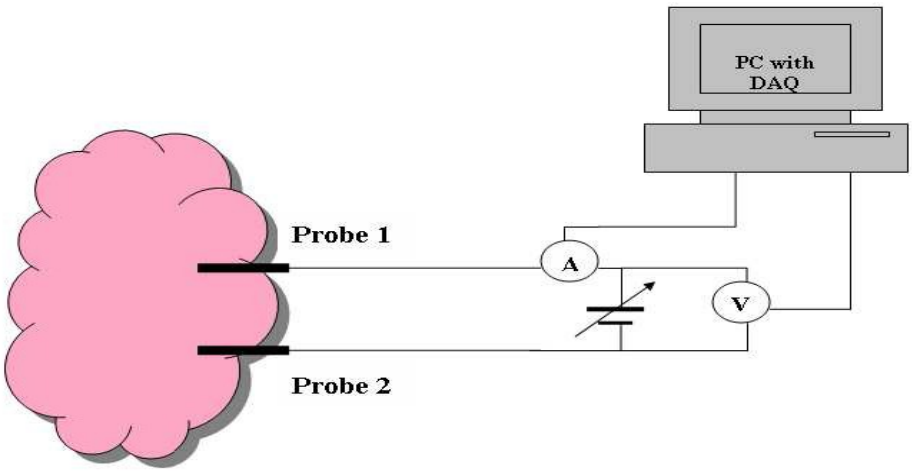


Figure 3.1: Electrical circuit for double probe measurement.[42]

It can be used for determining the electron temperature and the plasma density (from the ion saturation current). Under various conditions the double probes has been studied both theoretically and experimentally, by Johnson and Malter (1950), Cozens and Von Engel (1965), and Bardley and Mathews (1967)

[35, 36, 37] and several researchers as a tool for measurement of plasma characteristics. The double probe method (DP) make use of two probes, each similar to the single probe (SP). They are interconnected as shown in Fig.(3.1).

As in the (SP), the (DP) is based on the Boltzman relation and the plasma sheath properties of a gas discharge, and the electron temperature will be determined by the way in which $I_d$ (discharge current) varies with $V_P$ (probe voltage).

In this case, the probe current will be smaller than the discharge current. In addition, (DP) is based on an application of Kirchhoff's-current law which requires in this case that at any instant the total net current of positive ions and electrons flowing to the system from the plasma must be zero.

An idealized plot of the measured current as a function of the potential difference, as the latter changes from a fairly large value in one direction to a similar value in the opposite direction, is shown in Fig. (3.2). For simplicity it is assumed that the two probes are identical for our case, so that the two portions of the curve have the same shape.

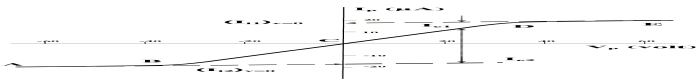

Figure 3.2: Characteristic of symmetric double probe.[16]

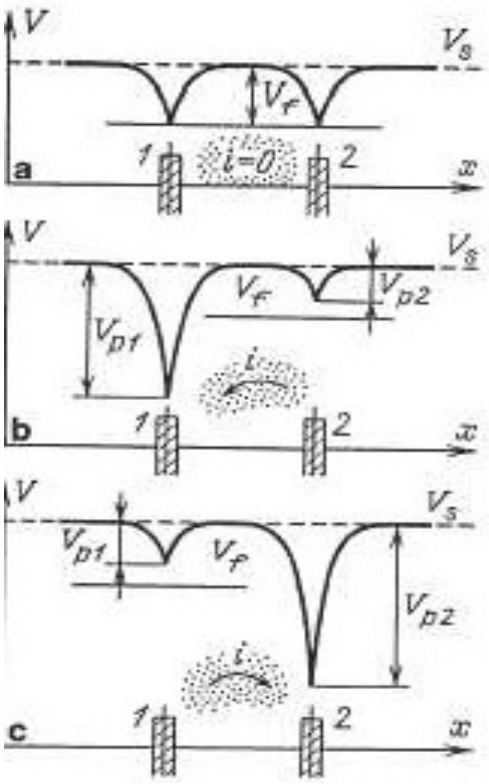


Figure 3.3: Double probe potential: (a)Floating potential, no current through the probes; (b) Left-hand probe is strongly negative, and receives ionic saturation current.(c) Polarity reversal; the right-hand probe is strongly negative[16].

Suppose the voltage applied from the battery is such as to make probe2, highly negative with respect to probe1. Probe2 will then collect positive ions at the maximum rate, so that the observed current is equal to $I_{i2}$, the random ion current to probe2. Probe1 will then collect an equivalent number of electrons, but no ions. However, since the ions are more slowly collected than the electrons, the maximum ion current can be measured, rather the maximum possible electron current, which determines the maximum (absolute) value of the current flowing through the plasma between the probes.

As the potential of probe 2 is made less negative in Fig. (3.2), the current remains constant along AB, but in the vicinity of B the potentials are such that some electrons, in addition to positive ions, are collected at probe2. The absolute magnitude of the net plasma current IP thus decreases B to C. At C, the external voltage between the probes is zero; both probes then have the same potential with respect to the plasma and no current flows Fig. (3.3a).

As the direction of the applied voltage is changed, the probe1 now becomes negative with respect to probe2 Fig. (3.3b), the situations is exactly reversed, and the curve CDE in Fig. (3.2) is obtained for the current $I_P$ , which now flows in the opposite direction Fig.(3.3c), as a function of the voltage $V_P$ applied between the probes. Thus, DE gives $I_{i1}$, the random ion current to probe1, and this will be the same as $I_{i2}$ if the probes are identical.

The total current to the system can never be greater than the saturation ion current, since any electron current to the total system must always be balanced by an equal ion current. Thus the disturbance on the discharge is minimized. This has the disadvantage, however, that only the fast electrons in the tail of the distribution can never be collected; the bulk of the electron distribution is not sampled.

The condition that the system be floating is:

$$I_{i1} + I_{i2} - I_{e1} - I_{e2} = 0 \qquad (3.1)$$

The current $I_P$ in the loop is given by

$$I_{i1} + I_{i2} - (I_{e1} - I_{e2}) = 2I_P \qquad (3.2)$$

If we add and subtract Eq. (3.1), and Eq. (3.2), we obtain:

$$I_P = I_{e1} - I_{i1} = I_{i2} + I_{e2} \qquad (3.3)$$

The current $I_e$ are given by

$$I_e = \frac{1}{4} n_e A \bar{v}_e \exp\left(-\frac{eV_f}{kT_e}\right) = n_e A \left(\frac{kT_e}{2\pi m}\right)^{1/2} \exp\left(-\frac{eV_f}{kT_e}\right) \qquad (3.4)$$

where n is the electron density, A is the probe area, $\bar{v}_e$ is the average electron velocity, $V_f$ is the floating potential, and $T_e$ is the electron temperature in $K^0$.

Calculated value for $R_L$ (Larmour radius) by Equation (3.5) for ions is $2.973 \times 10^{-4}$ m and $R_L$ for electrons is $1{,}297 \times 10^{-2}$ m.

Also, since $R_L$ is very small with respect to $\lambda_D$ (Debye length), which is proportional to $\left(\frac{T_e}{n_e}\right)^{1/2}$ in our case Eq. (3.4) is applicable.

$$R_L = \frac{mv_e}{eB} \tag{3.5}$$

.

For the electron current density to a probe in the transition region:

$$I_{e1} = A_1 j_{re1} \exp\left(-\frac{eV_1}{kT_e}\right) \tag{3.6}$$

and

$$I_{e2} = A_2 j_{re2} \exp\left(-\frac{eV_2}{kT_e}\right) \tag{3.7}$$

Here $I_{re} = Aj_{re}$ is the random electron current, and $j_{re}$ is the random electron current density. Substituting this into the first of Eq. (3.3) and using
($V = V_1 - V_2 > 0$), we have:

$$I_P + I_{i1} = A_1 j_{re1} \exp\left(-\frac{eV_1}{kT_e}\right) = A_1 j_{re1} \exp\left(-\frac{e(V+V_2)}{kT_e}\right) = \frac{A_1}{A_2} I_{e2} \exp\left(-\frac{eV}{kT_e}\right) \tag{3.8}$$

From the second part of Eq. (3.3),

$$\frac{I_P + I_i}{I_{i2} - I_P} = \frac{A_1}{A_2} \exp\left(-\frac{eV}{kT_e}\right) \tag{3.9}$$

The basic assumption of this theory is that the probes are always negative enough to be collecting essentially saturation ion current; therefore, $I_i$ can be accurately estimated at any V by a smoothly extrapolating the saturation portion of the double-probe characteristic.

Since we have probes with equal area ($A_1 = A_2$) then $I_i \approx I_{i1} \approx I_{i2}$, the formula:

$$I_P = I_i \tanh\left(\frac{V}{2T_{eV}}\right) + \frac{V}{R} + I_0 \qquad (3.11)$$

has been used [28, 38] to fit the experimental curve accurately for all of (TCDP), where R accounts for the effects of sheath expansion on probe current ($I_i$) as well as leakage current between the electrodes (due to the possible contamination), and $I_0$ account for any displacement current due to a time varying floating potential and the difference in stray capacitance to ground for each electrode.

However, our small correction to fit this formula to the I - V characteristics, which are shifted from the original point, is that:

$$I = I_P \tanh\left(\frac{(V - V_0)}{2T_{eV}}\right) + \frac{(V - V_0)}{R} + I_0 \qquad (3.12)$$

where $V_0$ is any constant, which can be fixed after getting a good result, then start the fit method "Levenberg -Marquardt algorithm" from the beginning.

Therefore, the electron temperature can be determined directly from the fit parameters [39].The electron density ne ≈ $n_i$ (assuming quasi-neutrality, and usually equal to the plasma density n), is obtained from the formula :

$$I_P = Ane^{3/2}\left(\frac{T_{eV}}{M_i}\right)^{1/2} \qquad (3.13)$$

where $T_{eV}$ is the electron temperature in eV , e is the electron charge, A is the probe tip area, and $M_i$ is the ion mass. The assumptions involved in the application of Eq. (3.2) are that the electron velocities are isotopic and Maxwellian, and that the sheath is collisionless. As the ratio ($rp/\lambda_D$) increases, Eq. (3.12) is no longer applicable [31, 40].

A Langmuir probe immersed in plasma will, under equilibrium conditions, assume a negative potential (the floating potential) with respect to the plasma, so that the random electron current density at the probe surface is attenuated from its bulk plasma value to a quantity equal to the random ion current density.

Then the floating potential $V_f$ is defined by $I_p = I_e$. Then by setting Eq. (3.4, and 3.12) equal yields:

$$V_f = -\frac{T_{eV}}{2}\ln\left(\frac{2M_i}{\pi m}\right) \qquad (3.14)$$

Since $V_f = 5T_e$ , the sheath is well established at this potential, and the expected

$I_i(V_f)$ can be calculated without the uncertainties inherent in extrapolation to the space potential $V_s(= 0)$ due to the weak ion accelerating field there[41].

# CHAPTER 4

# EXPERIMENTAL APPARATUS

## 4.1 Discharge Tube and Double Probe System

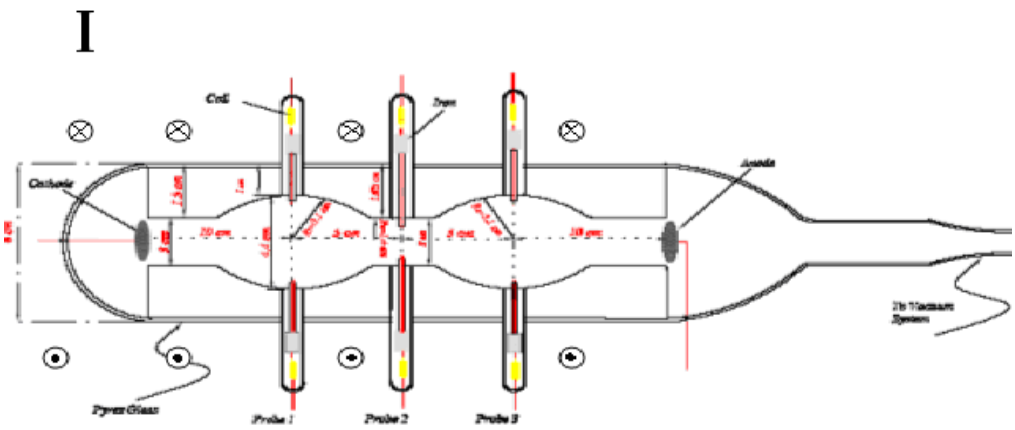


Figure 4.1: Schematic diagram of experimental apparatus.

Fig.( 4.1) is the schematic diagram of the apparatus used as a discharge reactor system which is made of pyrex glass. Since, discharge tube with variable diameters in the same system of glow discharge has not studied very well until now.

The outer glass is (uniform cylindrical) of length (30 cm) with inner diameter (5.6cm) and the internal one is (nonuniform) fixed to the external glass. It is constructed in a way that the diameter has been changed from the cathode to the anode but with symmetry in the middle point. The diameters for regions near electrodes are (4.2 cm), but in the middle is (2.8 cm). Argon has been used as a discharge gas, since it has the advantage of a relatively complete set cross section and a minimum of discharge chemistry.

Because of high melting point as well as low sputtering yield, the cylindrical type of tungsten wire has been used as a probe, and coated with capillary Pyrex tube. The tips of cylindrical double probes are equal in length (0.5 mm) with radius ($r_p$ = 0.0875 mm). An external adjustment method (magnetic effect on a cylindrical iron placed at the probe ports) has been used to change the radial position of the probes. The iron cylinder is covered with a glass tubing to avoid any chance of contamination in cell atmosphere. The moveable (TCDP) was inserted into the plasma through the orifice in the tube wall perpendicularly to the discharge axis, and they were fixed near the axis of internal discharge tube. The distance between each couple of probes is 5 cm in the axial direction.

Using one side of the each double probe as a fixed probe at the center and moving the other probe, the measurements of the radial potential gradient has been done at constant pressure (0.7 torr). Since, the distance between each couple of probe will not be very large (1.9 cm for probe 1 and 3, and 1.2 cm for probe 3) such that the plasma parameters could not different, where the probes are located.

A computer-controlled data acquisition (from National Instrument) has been employed for this work. The system consists of a compatible PC hosting a DAQ card (NI 6014, 16 bit and 200KS/s). The input voltage will be controlled by (DAC) (digital-to-analog converter), by generating the square wave. Therefore, the current from each probe is recorded for each voltage step at a sampling rate of up to 75 Hz [37].

The National Instrument (SC-2345) Series which is the enclosure for SCC signal conditioning modules connect directly to 68-pin ADQ device. The SCC-AO10 is an isolated voltage output module with an output range of ±10 V. The output voltage level is controlled by the DAC output of an E Series ADQ device using LabVIEW programme. This ±10 V will be amplified to a ±75 V output with

PA85 (high voltage operational amplifier) to the probe. The currents flowing in the probe circuit (there are three separate circuits) Fig.(4.2) and Fig. (4.3) can be detected using the (AD620) from Analog Device. It is a low cost, high accuracy instrumentation amplifier that requires only one external resistance to set gains (programmable gain with bandwidth 120 kHz at G =100) of 1 to 1000.

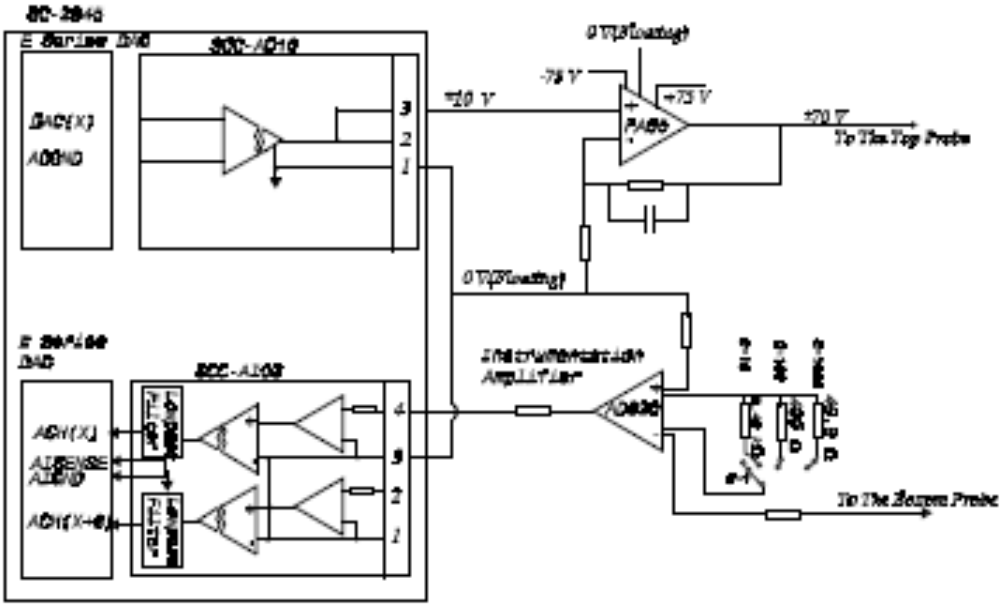

Figure 4.2: Schematic diagram of the double probe diagnostic system.[42]

Hence, the probe circuit has been developed, and can be used for magnetized plasma or slowly oscillating systems. In addition, the SCC- AI Series isolated analog input modules (SCC-AI03 with input impedance 100MΩ) can extract a relatively low-amplitude input signal from a high-common-mode voltage, so the E Series DAQ device can measure the input signals. It can also amplify and filter the input signal (with bandwidth 10 kHz), resulting in higher measurement resolution and accuracy. The inputs are designed in a floating (non-referenced) single-ended configuration. LabVIEW Express program has been used to control the whole system, and the three regions have been checked simultaneously in a very short time, approximately 0.5 ms for each probe.

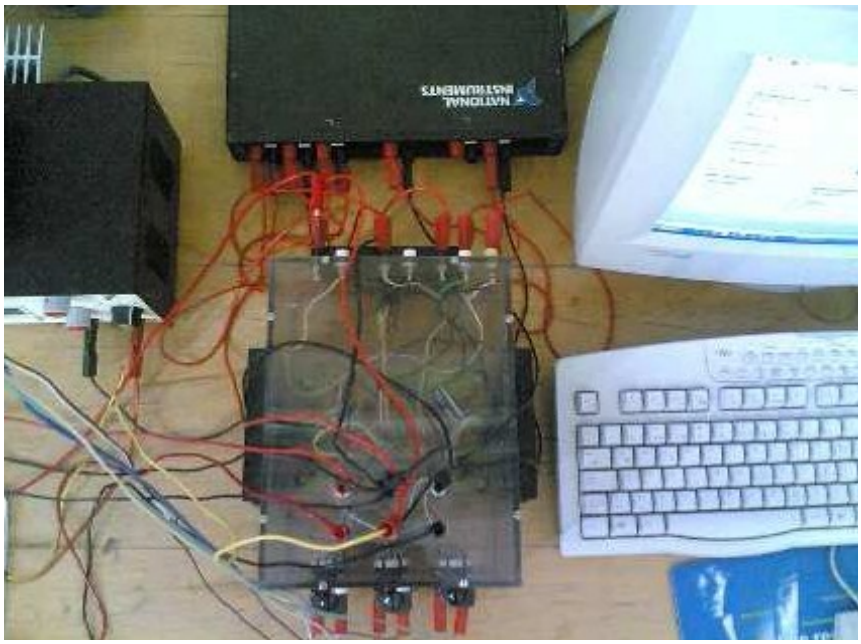


Figure 4.3: The electronic parts of the isolated computer controlled three couples of double probe (TCDP) system. [42]

### 4.2 The Pressure Measurement System

The experiments are performed using two-stage vacuum pump (mechanical and oil diffusion) to evacuate the whole system down to $10^{-4}$ torr. The chamber pressure was controlled with wide range gauge an MKS SensaVac Series 953 Pirani/Cold Cathode Ionization Vacuum Gauge (from $10^{-9}$ torr to atmosphere).

An analog-to- digital converter has been used as a digital gauge pressure with an input voltage (0-4 volt) for Pirani (for range until $10^{-4}$ torr) or (0-7 volt) for the cold cathode (for range $10^{-2}$ to $10^{-9}$ torr).

# CHAPTER 5

# RESULTS AND DISCUSSION

## 5.1 Current-Voltage Characteristics:

A series of (*I- V* ) measurements, as shown in Figs.( 5.1, 5.2, 5.3, 5.4, 5.5 , 5.6), demonstrating the effect of the low and high discharge currents, have been carried out to investigate the behavior of electric discharge in the tube over a certain range of argon gas pressures and discharge currents for all three double probes at the same time. Magnetic field is calculated according to formula (5.1)

$$B = \mu_0 nI \qquad (5.1)$$

where n=N(number of winding)/L(length of selenoid). In the experiment three different values of current is applied and therefore magnetic field has three different values.

$$B = \begin{cases} B1 = 2{,}97\ \ 10^{-2}\,T & for \quad I = 20\,A \\ B2 = 4{,}45\ 10^{-2}\,T & for \quad I = 30\,A \\ B3 = 5{,}94\ \ 10^{-2}\,T & for \quad I = 40\,A \end{cases}$$

Magnetic field values are classified with respect to their increasing values as B1, B2 and B3. All the three magnetic field values has two branches with two different discharge currents. The smallest magnetic field (B1) values with two different discharge current ($I_d$=5 mA and $I_d$=15 mA) affects in the same way as the largest valued magnetic field (B3). All measurements have been done at discharge currents ($I_d$ = 5 mA,  15 mA), and pressure ranges ($p$ = 0.3 – 2.1 torr), when the probes 1,3, and 2 are fixed radially at the distance 1.7 cm, and 1 cm from the wall of the inner tube, respectively.

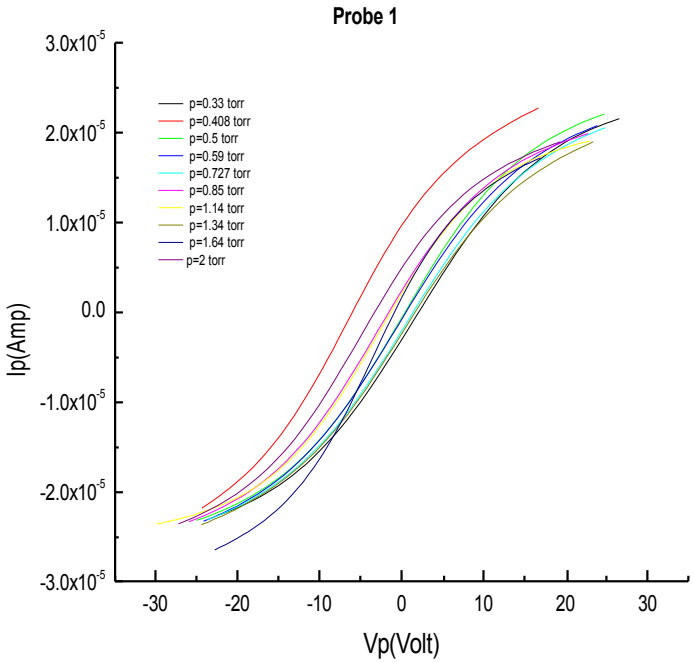
Probe 1
p=0.33 torr
p=0.408 torr
p=0.5 torr
p=0.59 torr
p=0.727 torr
p=0.85 torr
p=1.14 torr
p=1.34 torr
p=1.64 torr
p=2 torr
Ip(Amp)
Vp(Volt)
3.0x10-5
2.0x10-5
1.0x10-5
0.0
-1.0x10-5
-2.0x10-5
-3.0x10-5
-30
-20
-10
0
10
20
30

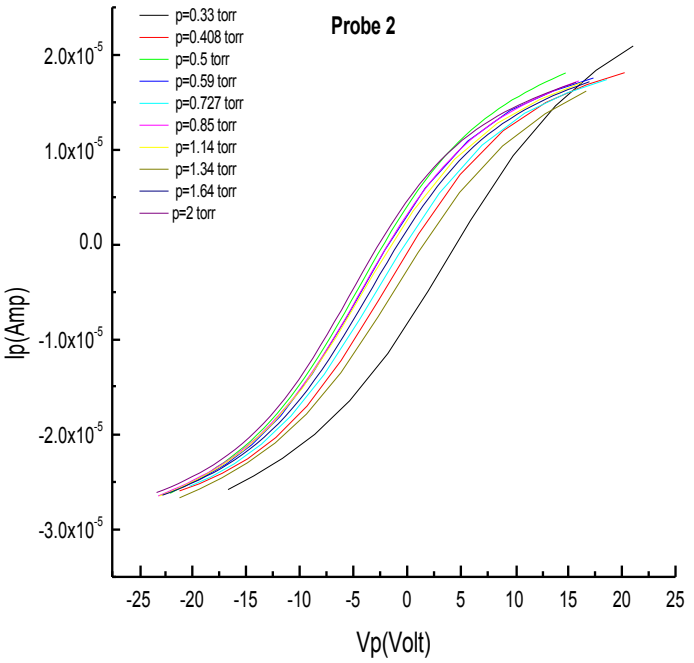
Probe 2
p=0.33 torr
p=0.408 torr
p=0.5 torr
p=0.59 torr
p=0.727 torr
p=0.85 torr
p=1.14 torr
p=1.34 torr
p=1.64 torr
p=2 torr
Ip(Amp)
Vp(Volt)
2.0x10-5
1.0x10-5
0.0
-1.0x10-5
-2.0x10-5
-3.0x10-5
-25
-20
-15
-10
-5
0
5
10
15
20
25

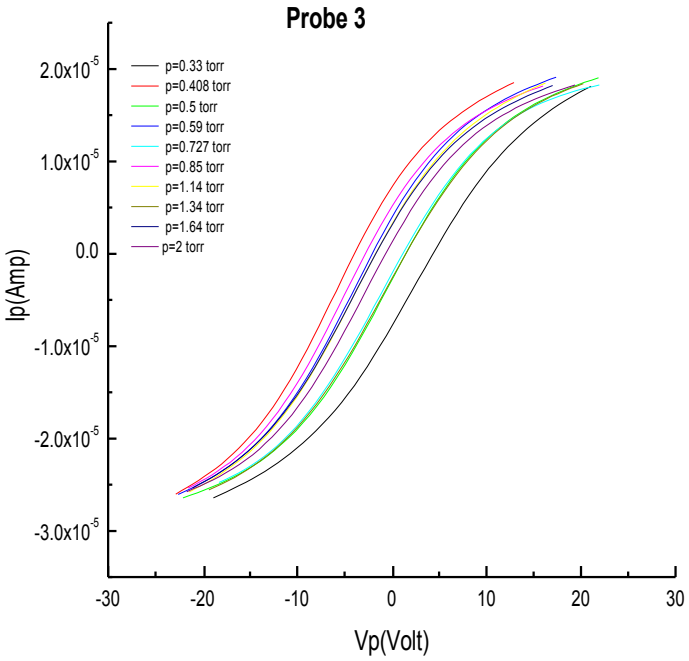


Figure 5.1: Double probe characteristic in argon gas at $I_d$ = 5 mA (at fixed radial distance (1.7 cm), and (1 cm) for probes 1, 3 and 2 respectively), and different pressures.(I=20 Amp B1)

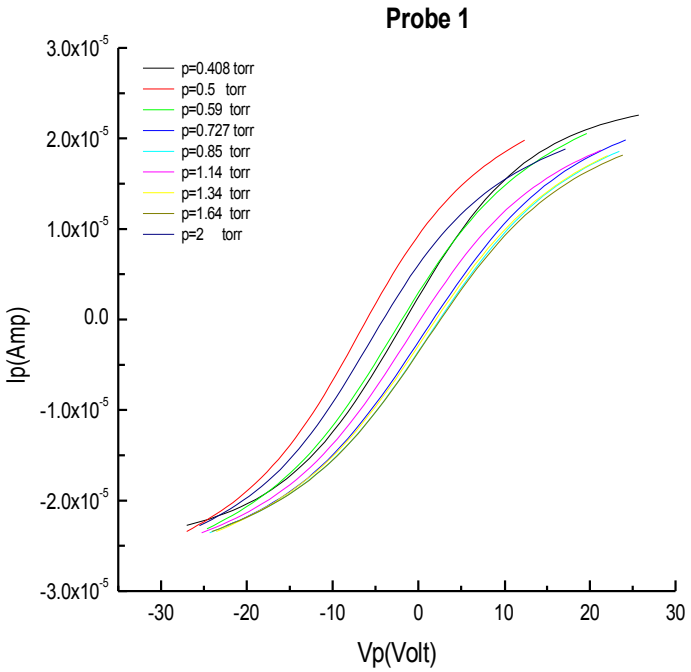
Probe 1
p=0.408 torr
p=0.5 torr
p=0.59 torr
p=0.727 torr
p=0.85 torr
p=1.14 torr
p=1.34 torr
p=1.64 torr
p=2 torr
Ip(Amp)
Vp(Volt)
3.0x10-5
2.0x10-5
1.0x10-5
0.0
-1.0x10-5
-2.0x10-5
-3.0x10-5
-30
-20
-10
0
10
20
30

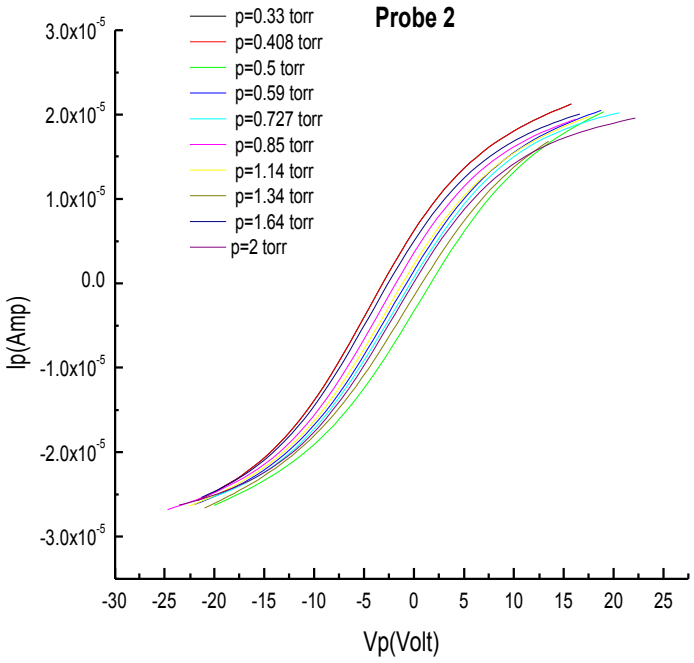
Probe 2
p=0.33 torr
p=0.408 torr
p=0.5 torr
p=0.59 torr
p=0.727 torr
p=0.85 torr
p=1.14 torr
p=1.34 torr
p=1.64 torr
p=2 torr
Ip(Amp)
Vp(Volt)
3.0x10-5
2.0x10-5
1.0x10-5
0.0
-1.0x10-5
-2.0x10-5
-3.0x10-5
-30
-25
-20
-15
-10
-5
0
5
10
15
20
25

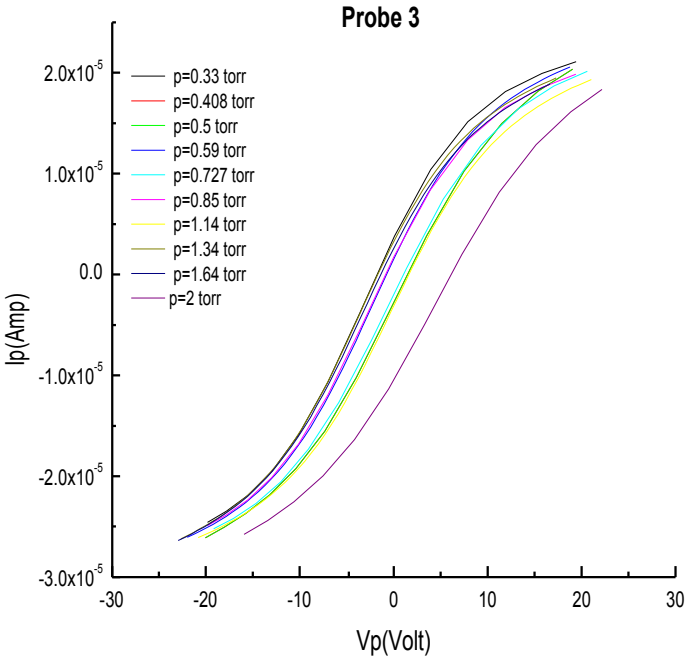


Figure 5.2: Double probe characteristic in argon gas at $I_d$ =15 mA (at fixed radial distance (1.7 cm), and (1 cm) for probes 1, 3 and 2 respectively), and different pressures.(B1)

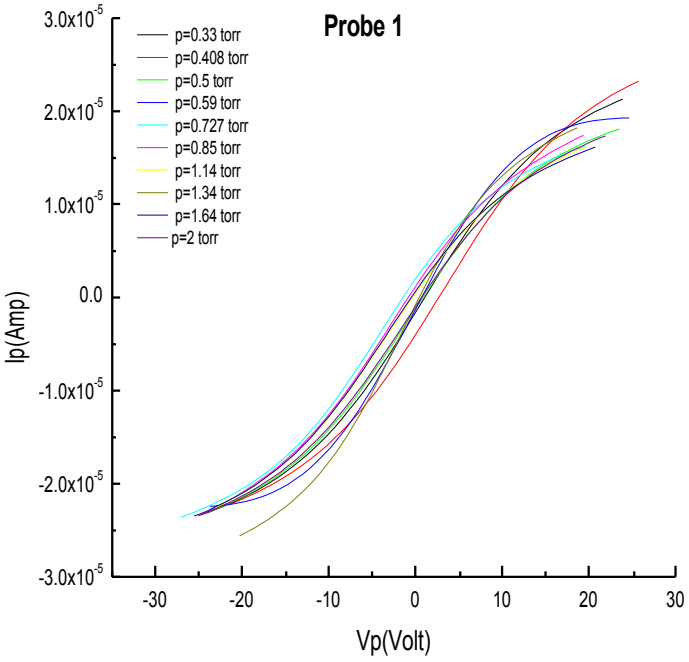

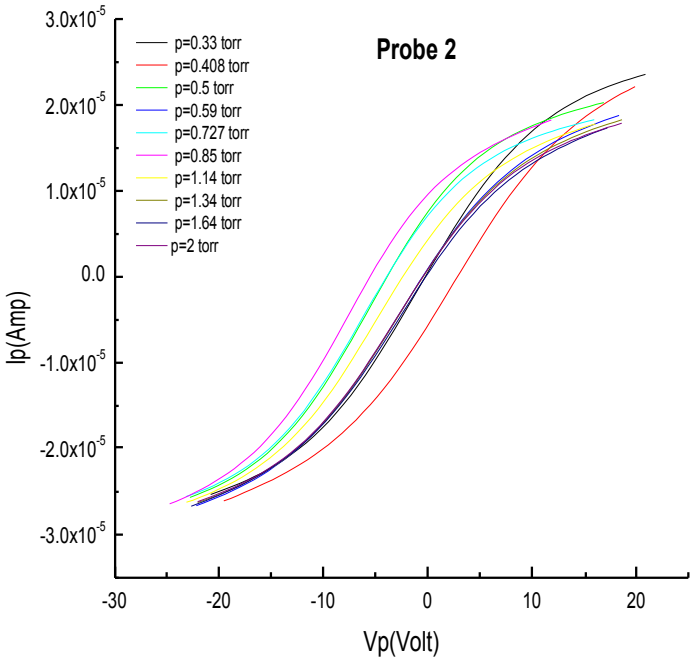


Figure 5.3: Double probe characteristic in argon gas at $I_d$ = 5 mA (at fixed radial distance (1.7 cm), and (1 cm) for probes 1, 3 and 2 respectively), and different pressures.(B2)

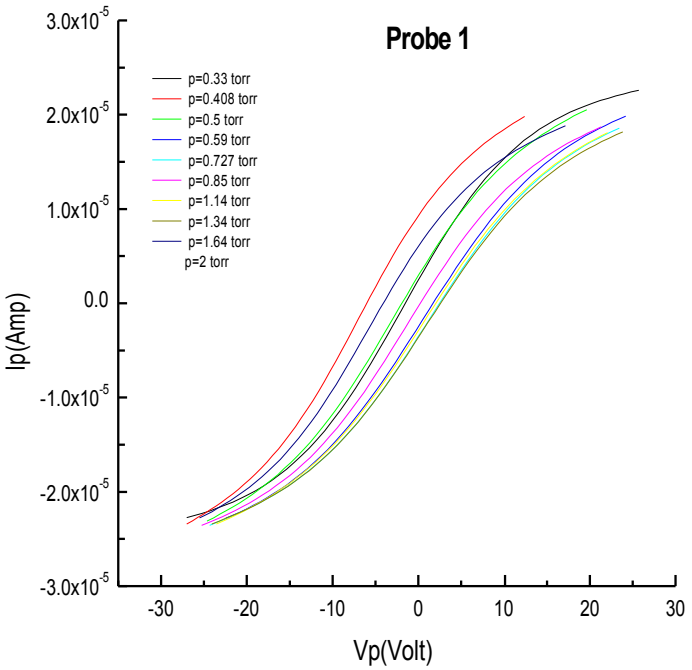
Probe 1
p=0.33 torr
p=0.408 torr
p=0.5 torr
p=0.59 torr
p=0.727 torr
p=0.85 torr
p=1.14 torr
p=1.34 torr
p=1.64 torr
p=2 torr
Ip(Amp)
Vp(Volt)
3.0x10-5
2.0x10-5
1.0x10-5
0.0
-1.0x10-5
-2.0x10-5
-3.0x10-5
-30
-20
-10
0
10
20
30

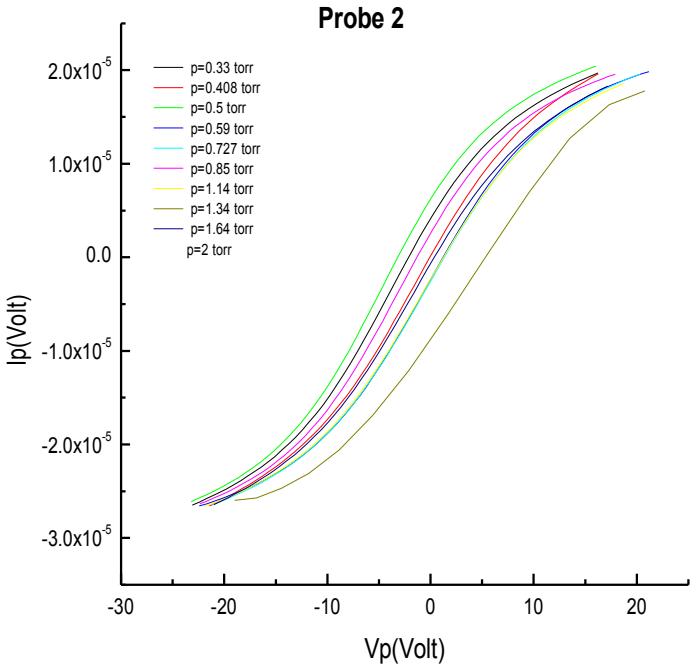
Probe 2
p=0.33 torr
p=0.408 torr
p=0.5 torr
p=0.59 torr
p=0.727 torr
p=0.85 torr
p=1.14 torr
p=1.34 torr
p=1.64 torr
p=2 torr
Ip(Volt)
Vp(Volt)
2.0x10-5
1.0x10-5
0.0
-1.0x10-5
-2.0x10-5
-3.0x10-5
-30
-20
-10
0
10
20

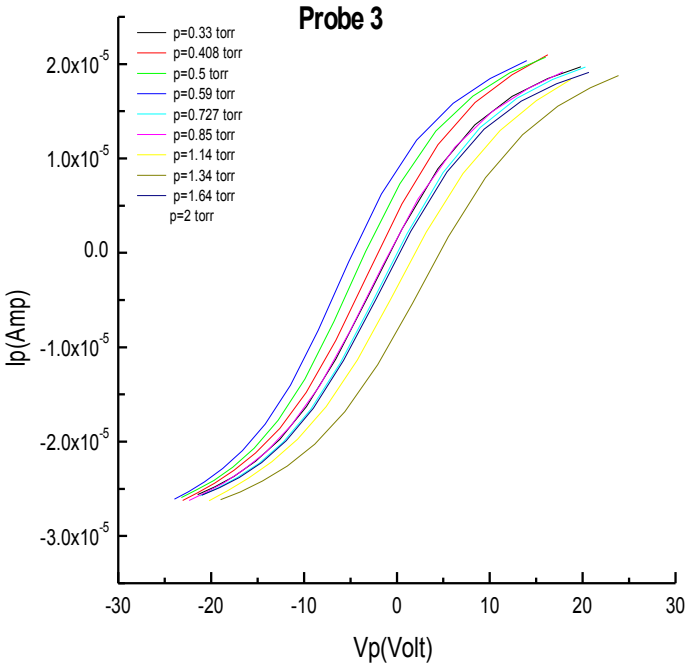


Figure 5.4: Double probe characteristic in argon gas at $I_d$ =15 mA (at fixed radial distance (1.7 cm), and (1 cm) for probes 1, 3 and 2 respectively), and different pressures.(B2)

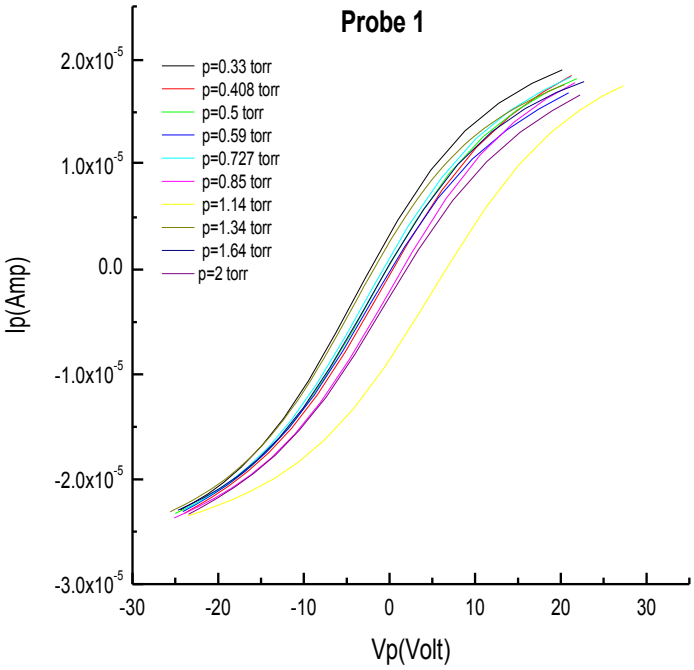

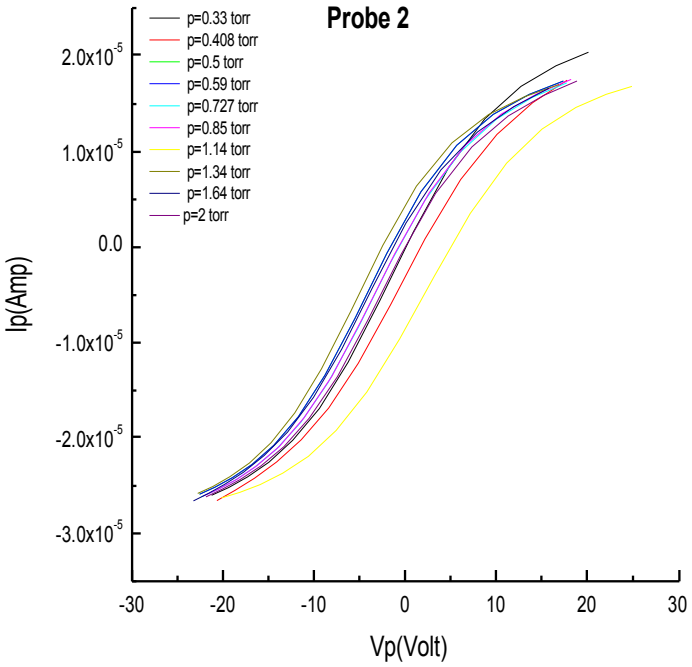


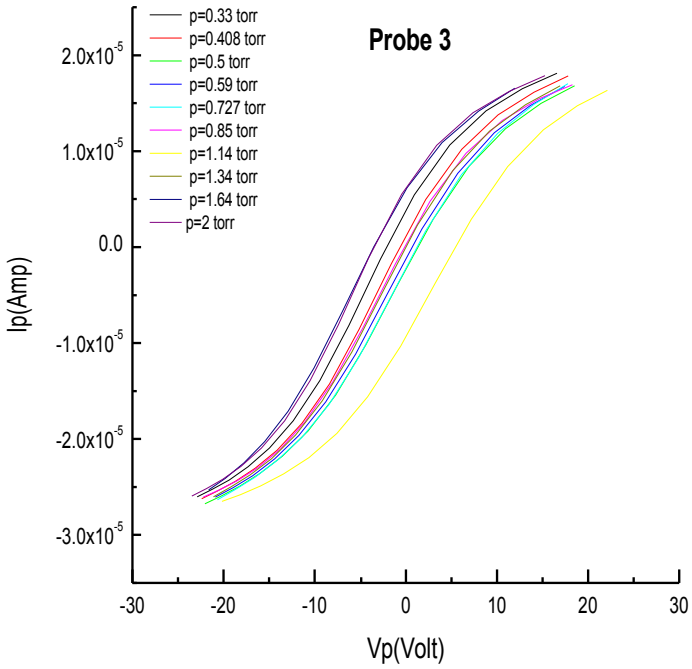


Figure 5.5: Double probe characteristic in argon gas at $I_d$ =5 mA (at fixed radial distance (1.7 cm), and (1 cm) for probes 1, 3 and 2 respectively), and different pressures.(B3)

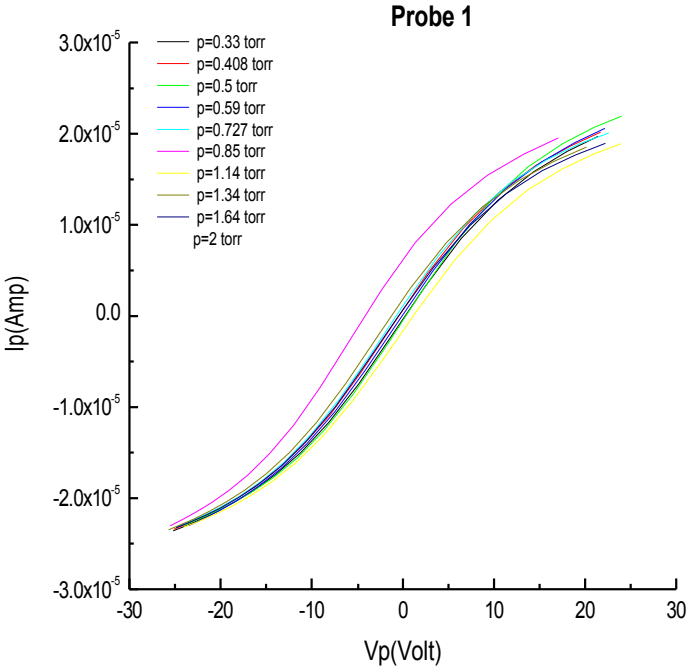
Probe 1
p=0.33 torr
p=0.408 torr
p=0.5 torr
p=0.59 torr
p=0.727 torr
p=0.85 torr
p=1.14 torr
p=1.34 torr
p=1.64 torr
p=2 torr
Ip(Amp)
Vp(Volt)
3.0x10-5
2.0x10-5
1.0x10-5
0.0
-1.0x10-5
-2.0x10-5
-3.0x10-5
-30
-20
-10
0
10
20
30

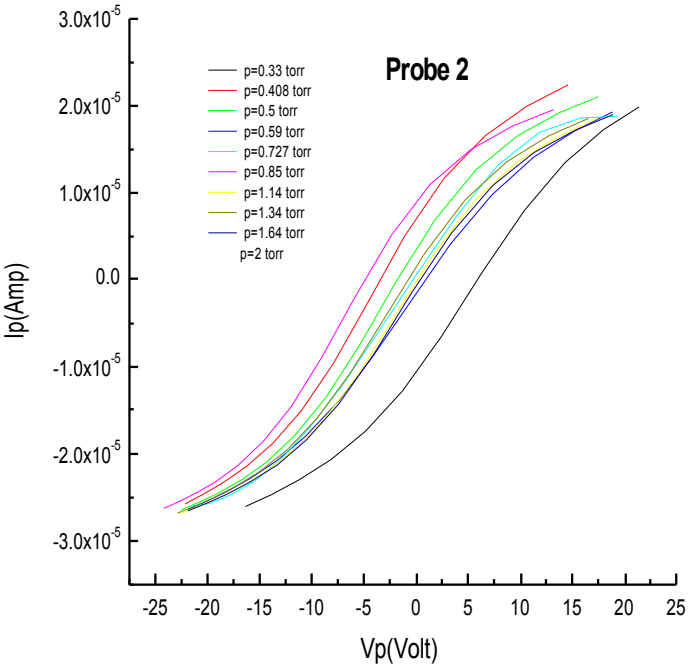
Probe 2
p=0.33 torr
p=0.408 torr
p=0.5 torr
p=0.59 torr
p=0.727 torr
p=0.85 torr
p=1.14 torr
p=1.34 torr
p=1.64 torr
p=2 torr
Ip(Amp)
Vp(Volt)
3.0x10-5
2.0x10-5
1.0x10-5
0.0
-1.0x10-5
-2.0x10-5
-3.0x10-5
-25
-20
-15
-10
-5
0
5
10
15
20
25

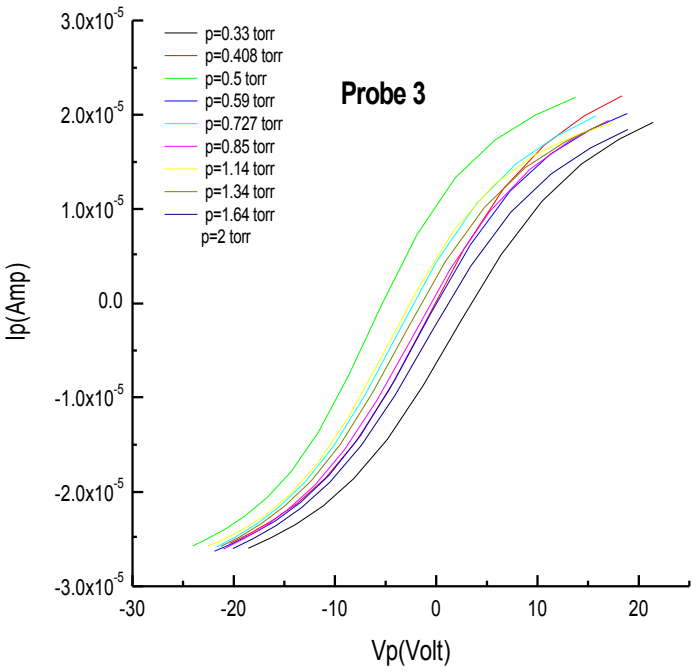


Figure 5.6: Double probe characteristic in argon gas at $I_d$ = 15 mA (at fixed radial distance (1.7 cm), and (1 cm) for probes 1, 3 and 2 respectively), and different pressures.(B3)

### 5.1.2 The Electron Temperature

$T_e$ variation of the electron temperature $T_e$ in argon gas for different values of the discharge current $I_d$ as a function of (pR); p is the gas pressure in torr and R is the tube radius are shown in figure 5.7,5.8, 5.9, 5.10, 5.11, 5.12.

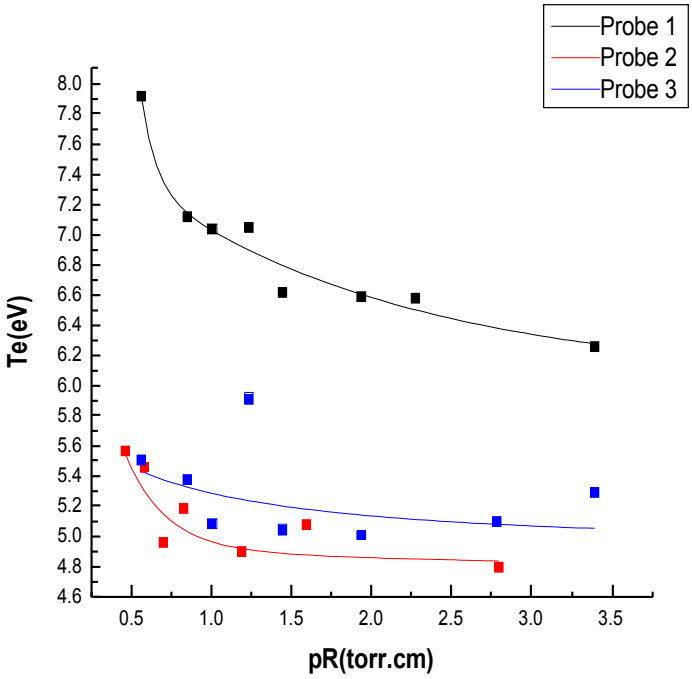


Figure 5.7: Electron temperature as a function of *pR* at discharge current $I_d$ =5 mA at fixed radial distance (1.7 cm), and (1 cm) for probes 1*;* 3 and 2 respectively. (B1)

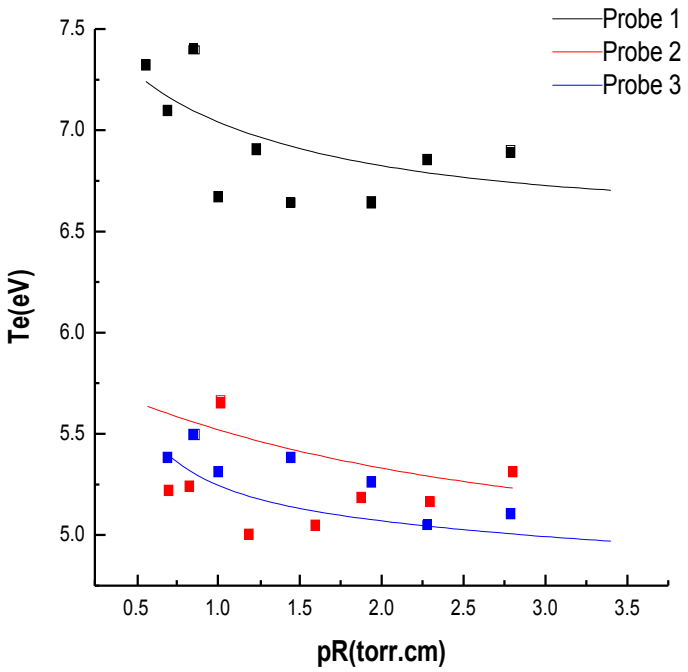


Figure 5.8: Electron temperature as a function of *pR* at discharge current $I_d$ =15 mA at fixed radial distance (1.7 cm), and (1 cm) for probes 1*;* 3 and 2 respectively.(B1)

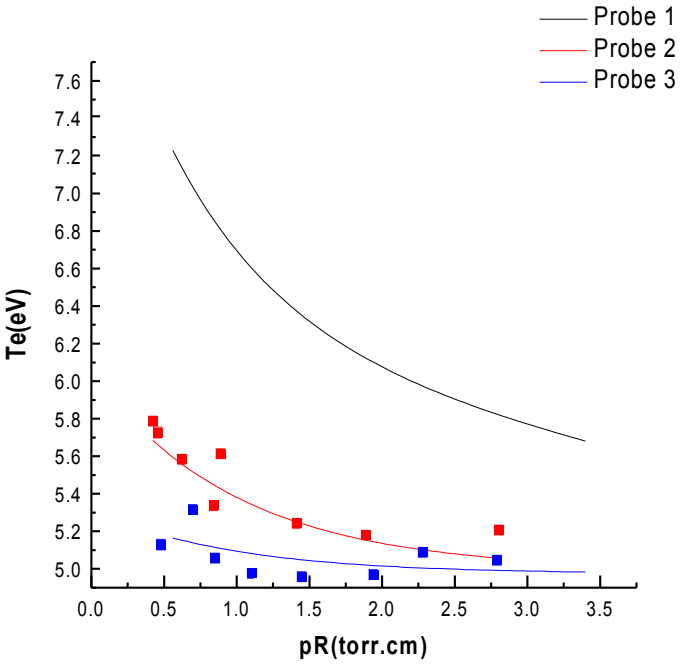


Figure 5.9: Electron temperature as a function of *pR* at discharge current $I_d$ =5 mA at fixed radial distance (1.7 cm), and (1 cm) for probes 1*;* 3 and 2 respectively.(B2)

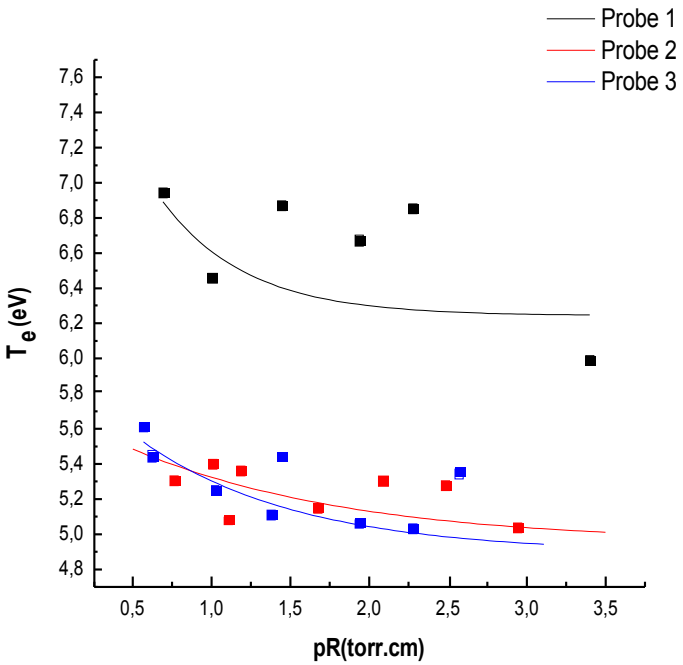


Figure 5.10: Electron temperature as a function of $pR$ at discharge current $I_d$ =15 mA at fixed radial distance (1.7 cm), and (1 cm) for probes 1*;* 3 and 2 respectively.(B2)

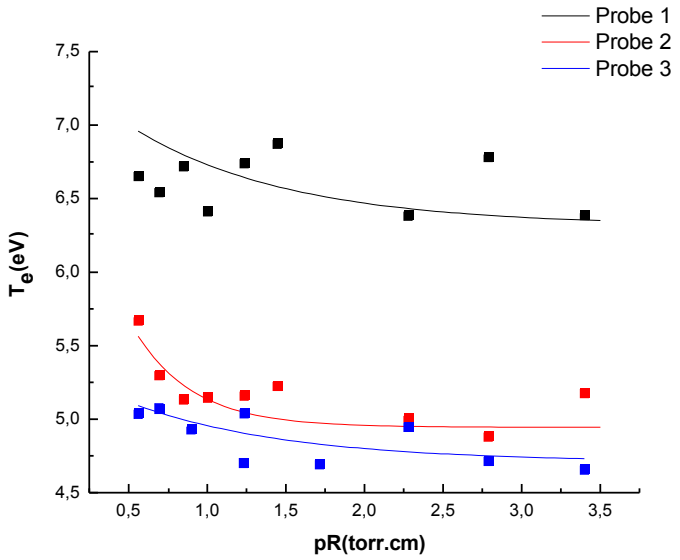


Figure 5.11: Electron temperature as a function of $pR$ at discharge current $I_d$ =5 mA at fixed radial distance (1.7 cm), and (1 cm) for probes 1*;* 3 and 2 respectively.(B3)

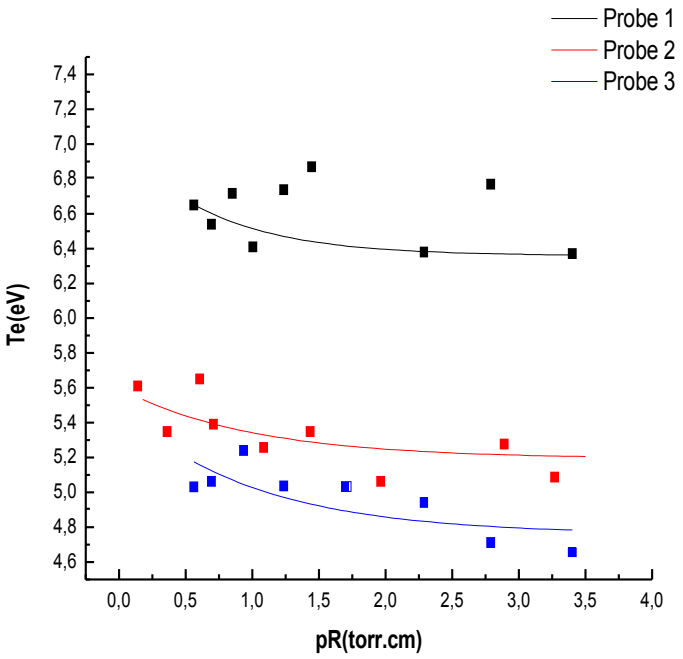


Figure 5.12: Electron temperature as a function of *pR* at discharge current $I_d$ =15mA at fixed radial distance (1.7 cm), and (1 cm) for probes 1*;* 3 and 2 respectively.(B3)

### 5.1.3 The Electric Field

Another important parameters, for the description of the positive column behavior is the axial electric field *E*. As can be seen from Fig.( 5.13, 5.14, 5.15, 5.16 , 5.17, 5.18). The electric field, in general, decreases with increasing *pR* values. Since, as the electron temperature decreases with increasing the pressure according to the ambipolar diffusion theory by Schottky [17], *E* tends to decrease as *pR* decrease.

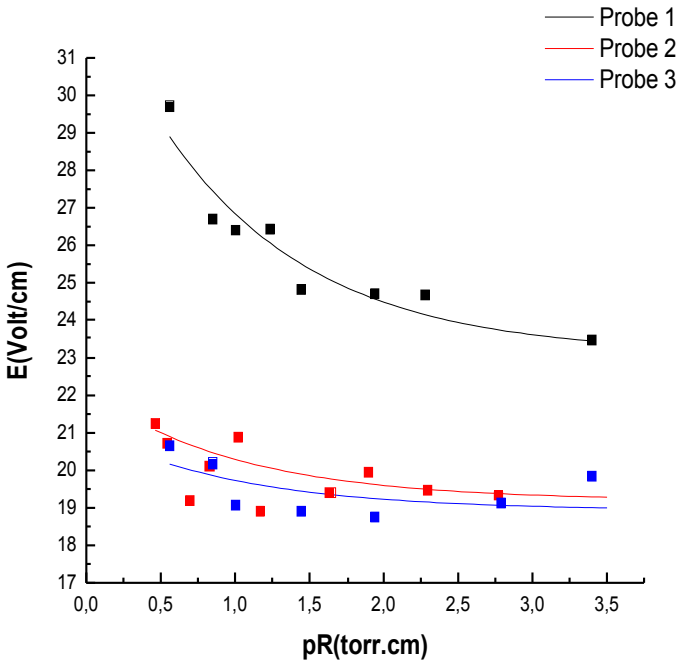


Figure 5.13: Axial electric field as a function of *pR* at discharge current (a) *Id* = 5 mA, (1 cm) for probes 1*;* 3 and 2 respectively.(B1)

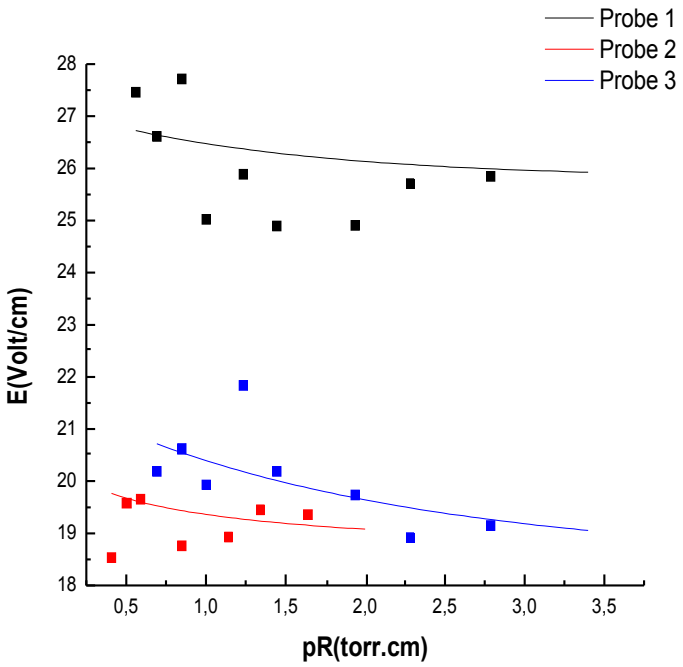


Figure 5.14: Axial electric field as a function of $pR$ at discharge current $I_d$ = 15mA, (at fixed radial distance (1.7 cm), and (1 cm) for probes 1, 3 and 2 respectively), and different pressures.(B1)

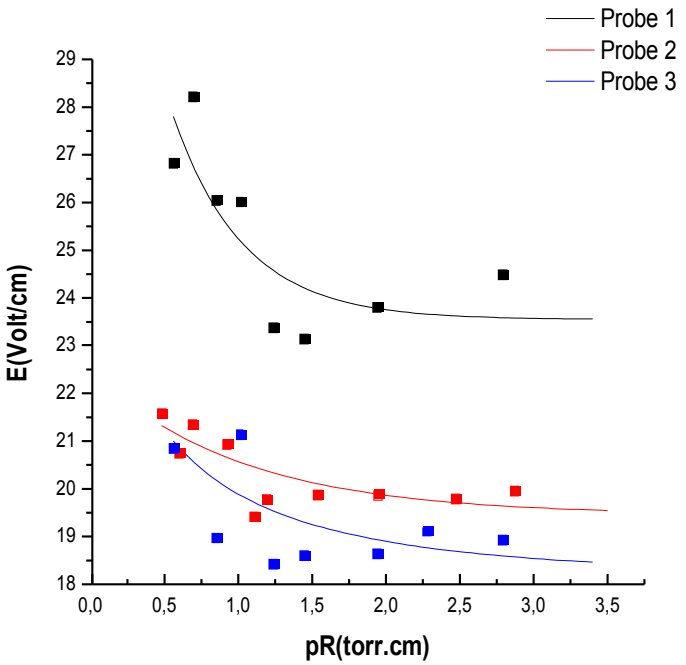


Figure 5.15: Axial electric field as a function of *pR* at discharge current $I_d$ = 5mA, (at fixed radial distance (1.7 cm), and (1 cm) for probes 1, 3 and 2 respectively), and different pressures.(B2)

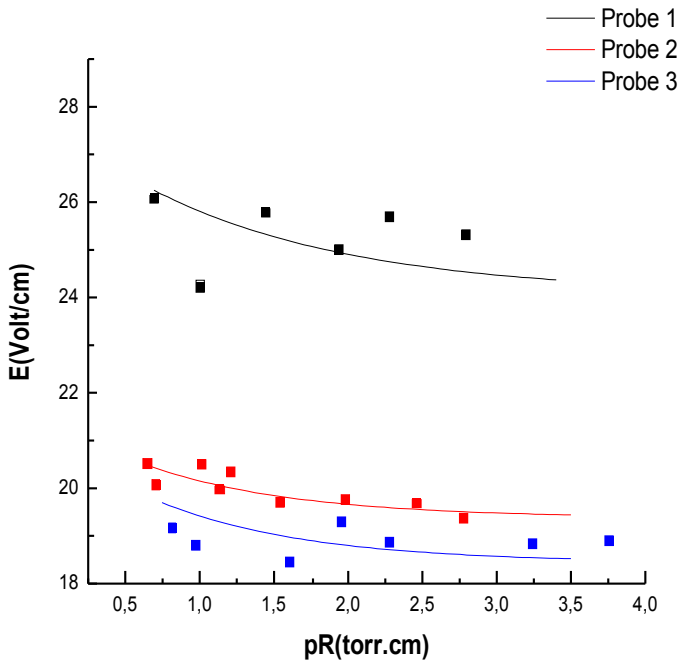


Figure 5.16: Axial electric field as a function of *pR* at discharge current $I_d$ = 15mA, (at fixed radial distance (1.7 cm), and (1 cm) for probes 1, 3 and 2 respectively), and different pressures.(B2)

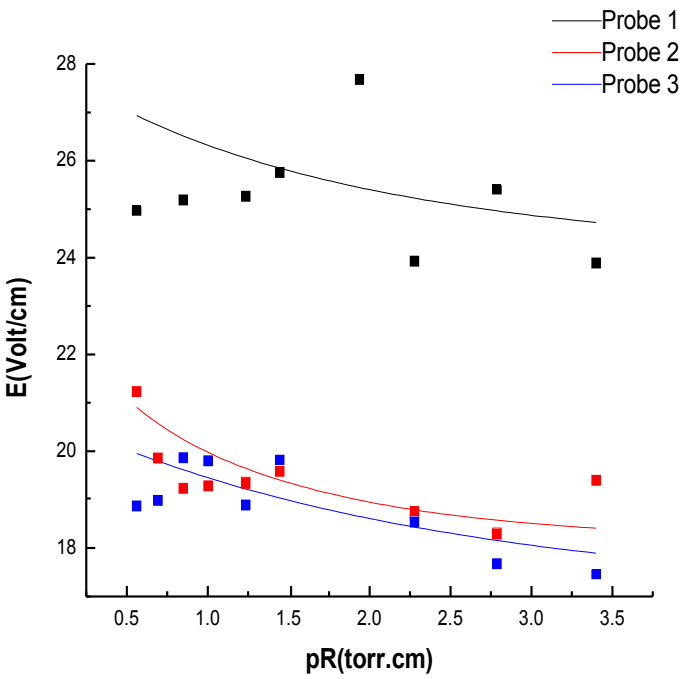


Figure 5.17: Axial electric field as a function of *pR* at discharge current $I_d$ = 5mA, (at fixed radial distance (1.7 cm), and (1 cm) for probes 1, 3 and 2 respectively), and different pressures. (B3)

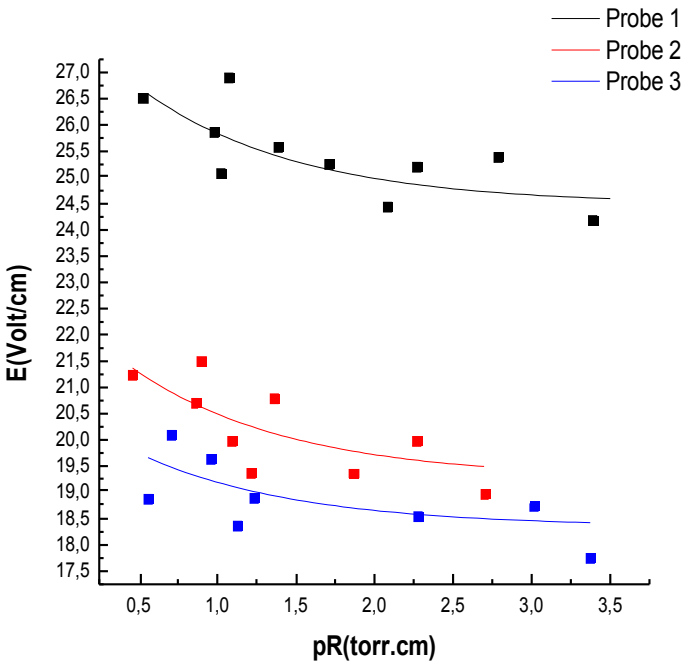


Figure 5.18: Axial electric field as a function of $pR$ at discharge current $I_d$ = 15mA, (at fixed radial distance (1.7 cm), and (1 cm) for probes 1, 3 and 2 respectively), and different pressures. (B3)

### 5.1.4 Electron Density

The variation of the electron density in argon gas for different values of the discharge current $I_d$ as a function of (pR); p is the gas pressure in torr and R is the tube radius are shown in figure 5.19, 5.20, 5.21, 5.22, 5.23, 5.24.

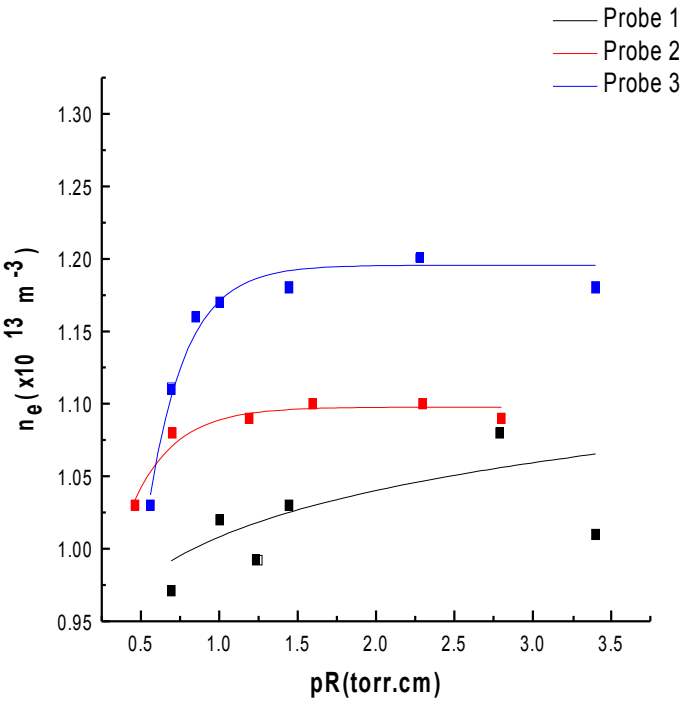


Figure 5.19: Electron density as a function of pR at discharges current Id = 5 mA at fixed radial distance (1.7cm), and (1 cm) for probes 1*;* 3 and 2 respectively. (B1)

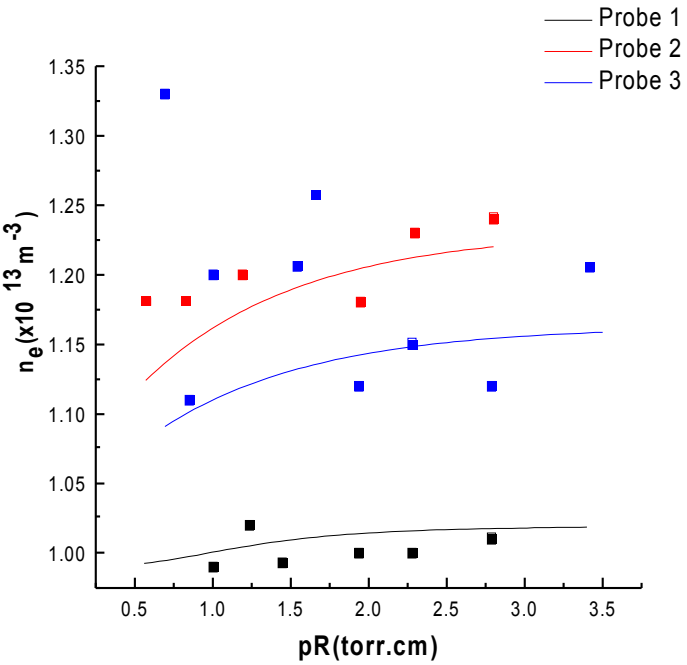


Figure 5.20: Electron density as a function of pR at discharge current Id = 15 mA at fixed radial distance (1.7cm), and (1 cm) for probes 1; 3 and 2 respectively (B1)

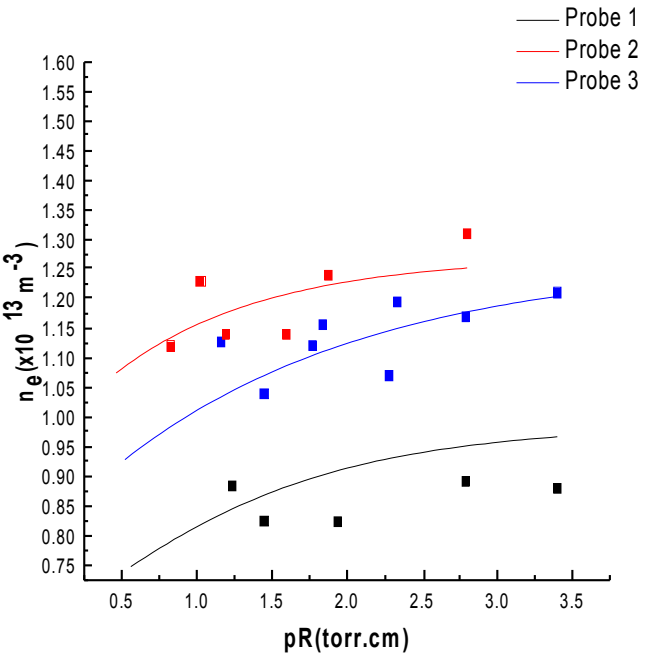


Figure 5.21: Electron density as a function of pR at discharge current Id = 5 mA at fixed radial distance (1.7cm), and (1 cm) for probes 1; 3 and 2 respectively (B2)

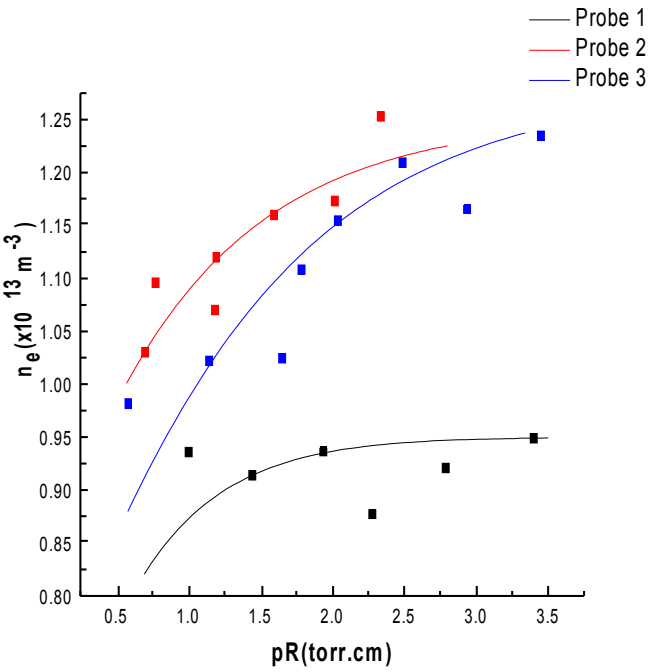


Figure 5.22: Electron density as a function of pR at discharge current Id = 15 mA at fixed radial distance (1.7cm), and (1 cm) for probes 1*;* 3 and 2 respectively (B2)

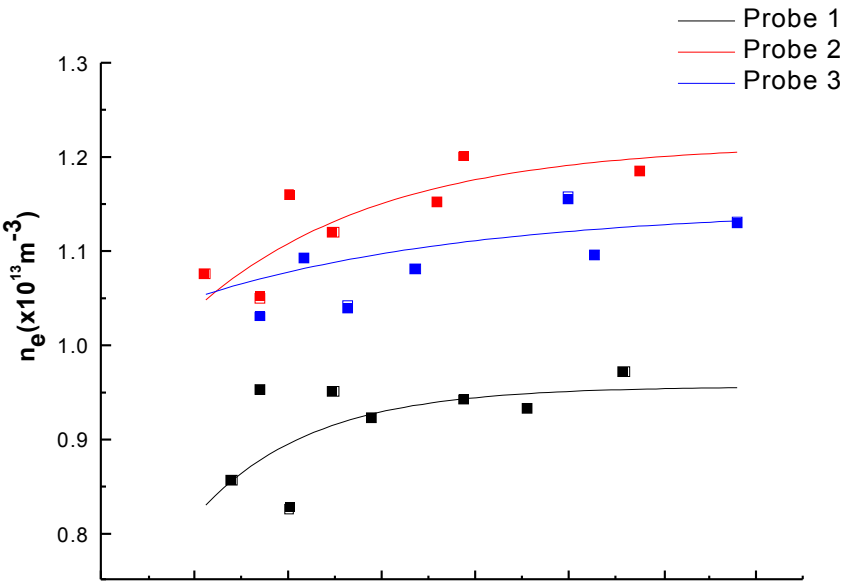


Figure 5.23: Electron density as a function of pR at discharge current Id = 5 mA at fixed radial distance (1.7cm), and (1 cm) for probes 1*;* 3 and 2 respectively (B3)

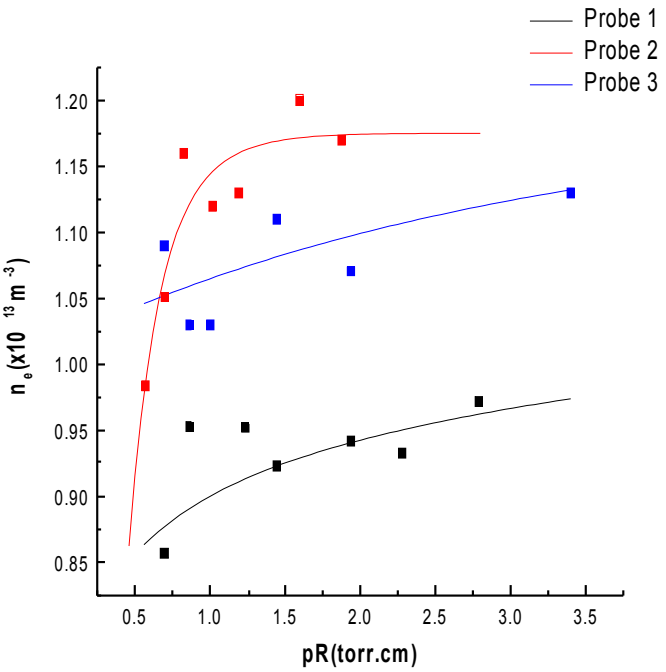


Figure 5.24: Electron density as a function of pR at discharge current Id = 15 mA at fixed radial distance (1.7cm), and (1 cm) for probes 1; 3 and 2 respectively (B3)

# CHAPTER 6

# CONCLUSION AND DISCUSSION

## 6.1 Conclusion

The non-uniform positive column argon DC glow discharge plasma has been investigated experimentally. To measure all plasma parameters, the computerized three dual Langmuir probe array set-up has been used with optically isolated circuit. This is to prevent stray capacitance to ground which can be a major source of error at the turn-on and turn-on transients. With 10 kHz low-pass filters a very good resolution and accuracy have been measured, and give a possibility to use it in a magnetized plasma and low frequency oscillating plasma systems.

The effect of the magnetic field is discused, and it is seen that Schottky theory well describes the spread positive column. It can be seen from the Figures 5.20, 5.22, 5.24 that at high discharge currents and low prossure values the positive column spreads laterally to the wall. It can be observed from the Figures 5.8, 5.10, and 5.12 that the magnetic field reduces the electron temperature from the value given by the Langmuir curve to that given by the Schottky theory. [42, 43]

The results of *I-V* measurements, which can be seen from Fig. (5.1, 5.2, 5.3, 5.4, 5.5, and 5.6) demonstrate that as the pressure increases the characteristic curve will shift toward the negative direction. The current-voltage characteristic has been shifted toward the negative direction with increasing the pressure, and the probe current in the double probe technique decreases with the increasing *pR*.

The result of $T_e$ *as a function of pR* measurements, which can be seen from Fig. (5.7, 5.8, 5.9, 5.10, 5.11, and 5.12) demonstrates that the electron temperature for all regions tends to decrease as the product pR increases. The electron temperature decreases with increasing pR and increasing magnetic field decreases generally their values.

Generally for the different magnetic field values, there exists a tendency for Probe 1 that this probe has greater values compared to the Probe 2 and Probe 3 but in the case of without magnetic field this difference between the probes can not be observed [42]. The order of electron temperature values from highest to lowest is P1>P3>P2 for discharge current value 5 mA and magnetic field value B1 but for all the other cases the order is like P1>P2>P3. We observed that the electron temperature values decreased with increasing discharge currents for all the three probes.

Another important parameters, for the description of the positive column behavior is the axial electric field *E*. As can be seen from Fig.( 5.13, 5.14, 5.15, 5.16 , 5.17 and 5.18), the electric field, in general, decreases with increasing *pR* values. Since, as the electron temperature decreases with increasing the pressure according to the ambipolar diffusion theory by Schottky [17], *E* tends to decrease as *pR* decrease.

Generally, the electric field values, for the different magnetic fields (B1, B2 and B3) have a tendency that the electric field at Probe 1 has greater values compared to the Probe 2 and Probe 3 but in the case of without magnetic field this difference for electric field values between the probes can not be observed [42]. The order of electric field values from highest to lowest is P1>P2>P3 for all cases. We observed that the electric field values decreased with increasing discharge current.

The variation of the electron density in argon gas for different values of the discharge current $I_d$ as a function of (pR); p is the gas pressure in torr and R is the tube radius are shown in Fig. ( 5.19, 5.20, 5.21, 5.22, 5.23 and 5.24). The common trends of the curves are that the electron density for all regions tends to increase as the product pR increases. The electron density for all regions tends to increase as the product of pR increases.

Generally, the electron density values for the different magnetic fields (B1, B2 and B3) have a tendency for Probe 1 that, this probe has smaller values compared to the Probe 2 and Probe 3 but in the case of without magnetic field this difference for electron density values between the probes can not be observed [42]. The order of electon density values from highest to lowest is P2>P3>P1 except for discharge current value 5 mA and magnetic field value B1 (For this case

P3>P2>P1). Also we observed that the electron density values increased with increasing discharge currents for all the three probes.

Work on this thesis can be continued in the future with:

1- Developing the measurement technique to be more fast and more electronically controlled.

For example, using programmable switches to control the gains.

2- Using different gases and its mixtures.

3- Using *RF* power instead DC power to get *RF* plasma.

4- Using conducting metallic wall instead of glass wall to study the plasma wall interaction.

## REFERENCES

[1] Perspectives on Plasmas, www.plasmas.org/applications.html, (last accessed date 11.05.2006)

[2] Plasma Science: From Fundamental Research to Technological Applications, Contributor: National Research Council, Panel on Opportunities, National Academies Press, (1995)

[3] Electron Kinetics and Applications of Glow Discharges: Proceedings of a Nato ARW held in St. Petersburg, Russia, May 19-23, (1997)

[4] National Research Council Staff. Plasma Processing of Materials: Scientific Opportunities and Technological Challenges.Washinton, DC, USA: National Academic Press, p8. (1991),

[5] J. Smith, IEEE Trans. Electron Devices ED-20, 1103, (1973).

[6] Y. Okamoto, Japan. J. Appl. Phys. 15, 719, (1976).

[7] T. Kaneda, J. Phys. D: Appl. Phys. 23, 500, (1989).

[8] C. Wilke, B. P. Koch, and B. Bruhn, Physics of Plasmas 12, 3350, (2005).

[9] W. Tao, and H. K. Yasuda, Plasma Chem. and Plasma Processing 22, 297, (2002).

[10] E. Hintz, 3rd Workshop on Plasma and Laser Technology, Ismailia, (1993).

[11] C. M. Anderson, W. G. Graham, and M. B. Hopkins, Appl. Phys. Lett. 52, 783, (1988).

[12] A. Von Engel, Ionized Gas, Oxford: Oxford University Press, (1965).

[13] J.J. Thomson and G.P. Thomson, Conduction of Electricity through gases Volume II., Dover Publications, (1969)

[14] J. D. Cobine, Gaseous Conductors, Theory and Engineering Application, Dover Publications Inc., New York, 2nd edition, (1958).

[15] A.M. Howatson, An Introduction to gas discharges, Pergamon Press, (1965)

[16] Yuri P. Raizer, Gas Discharge Physics, Spring Verlag, (1987).

[17] R. N. Franklin, Plasma Phenomena in Gas Discharges, Clarendon Press. Oxford,(1976).

[18] D. Akbar, and S. Bilikmen, Development of Computer Controlled Double Probe and Discharge System with Varying Diameters, 14th International

Conference on Surface Modification of Materials by Ion Beams (SMMIB), Kusadasi, Turkey, 04 Sept. 2005.
[19] D. Akbar, and S. Bilikmen, Fast Double Probe Technique and Effect of Non-Uniform Glow Discharge System on Plasma Parameters, 23th International Physics Congeress (TPS), Mugla, Turkey, 13-16 Sept. 2005.
[20] W. Schottky, Z. Phys. 25, 635, (1924).
[21] Ingold J H 1997 Phys. Rev. E. 56 5932.
[22] Loffhagen D., and Gorchakov S 2005 "Self-consistent Modeling of the Column Plasma of Low-pressure Glow Discharges", XXV IIth ICPIG, Eindhoven, the Netherland, July 18-22.
[23] A. V. Pheleps, and S.C. Brown, Phys. Rev. 13, 1202, (1952).
[24] H. J. Oskan, Philips Res. Rep. 13, 335, (1958).
[25] J. P. Graur, and L. M. Chainin, Phys. Rev. 182, 167, (1969).
[26] Y. Ichikawa, and S. Teii, J. Phys. D:Appl. Phys. 13, 2031, (1980).
[27] P. M. Chung, L. Talbot, and K. J. Touryan, Elecrostatic Probes in Sationary and Flowing Plasmas, Springer-Verlag, New York, (1975).
[28] F. F. Chen, Plasma Diagnostic Techniques, Academic Press INC., New York, (1965).
[29] J. D. Swift, and M. J. R. Schwar, Electrical Probes for Plasma Diagnostics, American Elsevier, New York, (1969).
[30] H. M. Mott-Smith, and I. Langmuir, Phys. Rev. 28, 727, (1929).
[31] F. F. Chen, Phys. Plasma 8, 3029, (2001).
[32] J. E. Allen, Phys. Scr. 45, 497, (1992).
[33] J. H. Rogers, J. S. De Groot, and D. Q. Hwang, Rev. Sci. Instrum. 63, 31, (1992).
[34] F. F. Chen, Langmuir Probe Diagnostics, Mini-Course on Plasma Diadnos-tics, IEEE-ICOPS meeting, Jeju, KOrea, (2003).
[35] E.O. Johnson, and L. Malter, Phys. Rev. 80, 58, (1950).
[36] J.R. Cozens, and A. Von Engle, Int. J. Electron 19, 61, (1965).
[37] D. Bardley, and K. J. Mathews, Phys. Fluids 10, 1336, (1967).
[38] B. A. Smith, and L. J. Oreizet, Plasma Source. Sci. Technol. 8, 82, (1999).
[39] D. Akbar, and S. Bilikmen, J. Appl. Phys. D: Appl. Phys. (2006)(submitted).
[40] D. S. Isaac , and W. R. Claude , J. Appl. Phys. 76, 4488, (1994).

[41] Francis F. Chen, John D. Evans, and Arnush, D., Phys. Plasmas 9, 1449,(2002).

[42]D.Akbar,The Non-Uniform Argon DC Glow discharge system parameters measured with fast three couples of double probes, PhD Thesis,(2006)

[43] R.J.Bickerton, A.Von Engel, The Positive Column in a Longitudinal Magnetic Field , Phys.Soc.,468, (1955)

[44] M.A. Lieberman, A. J. Lichtenberg "Principles of Plasma Discharges and Materials Processing" John Wiley, (1994)